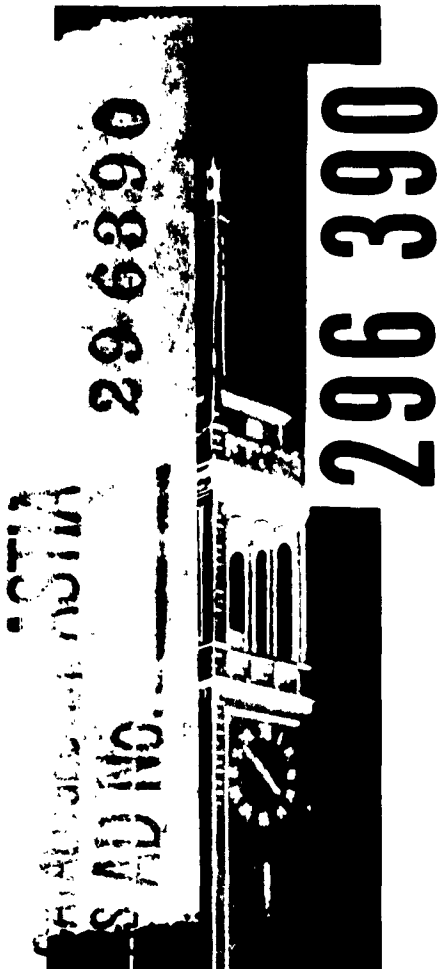

Plasma Oscillations and Particle Trajectories in a Drifting Electron Stream; Palmer Diagrams

by

C. K. Birdsall

Series No. 60, Issue No. 458
Contract No. AF 49(638)–102
June 29, 1962

ELECTRONICS RESEARCH LABORATORY

UNIVERSITY OF CALIFORNIA
BERKELEY CALIFORNIA

Electronics Research Laboratory
University of California
Berkeley, California

PLASMA OSCILLATIONS AND PARTICLE TRAJECTORIES IN A DRIFTING ELECTRON STREAM; PALMER DIAGRAMS

by

C. K. Birdsall

Institute of Engineering Research
Series No. 60, Issue No. 458

Physics Division
Air Force Office of Scientific Research
Contract No. AF 49(638)-102
Division File No. 13-25-J

June 29, 1962

ABSTRACT

Electron trajectories are obtained for the Hahn-Ramo space-charge waves. The approach is to use Lagrangian form of hydrodynamic equations of motion and of continuity. This is in contrast with the more common Eulerian jellied-out fluid approach where the particle identity is lost. The model used is developed in some detail. Trajectory plots are given for the faster and slower space-charge waves by themselves and for velocity modulation for the ratios of driving frequency to plasma frequency, ω/ω_p, of 0.5, 1.0, and 2.0.

TABLE OF CONTENTS

FUNDAMENTAL EQUATIONS, MODEL

In one formulation of the Lagrangian form of hydrodynamic equations, the independent variables are the time, t, and the initial (t = 0) coordinates of any particle of the fluid, say a, b, c. The dependent variables are the particle coordinates, say x, y, z; their values in terms of a, b, c, t give the whole history of every particle of the fluid. The components of velocity and acceleration of a given particle are given by:

$$\frac{\partial x}{\partial t}, \frac{\partial y}{\partial t}, \frac{\partial z}{\partial t} \text{ and } \frac{\partial^2 x}{\partial t^2}, \frac{\partial^2 y}{\partial t^2}, \frac{\partial^2 z}{\partial t^2},$$

respectively. Hence, the x component of the equation of motion is

$$m \frac{\partial^2 x}{\partial t^2} = F_x \tag{1}$$

where F_x is given at the position of the particle. m is the particle mass. The equation of continuity is not the same as that in the Eulerian formulation.

The quantities a, b, c need not be the initial coordinates of a particle, but may be any three quantities which serve to identify a particle and which vary continuously from one particle to another. In the one-dimensional model to be used here it is desired to obtain the trajectories of particles beyond the plane of injection say, x = 0. Each particle will be identified by its <u>time</u> of departure from x = 0, the a^{th} particle by t_a, etc. Thus for the a^{th} particle $x = x(t, t_a)$. The result is to be a plot of particle position as a function of time t, such as shown in Figure 1.

The notion of a particle <u>per se</u> in a continuous fluid may present some difficulty in conception. Of course, in a fluid of electrons and ions, one might be tempted to ask for the history of each charged particle; however, this request is absurd as there may easily be 10^{20} particles in a given problem. An alternative is to follow selected elements. The selection must be made with some care in order to obtain correct results.

In the continuous (Eulerian) fluid model, the dependent variables, v, ρ, i, describing the electron motion, can be shown to vary with time as $\cos \omega_p t$ as seen by an observer riding with the stream at average

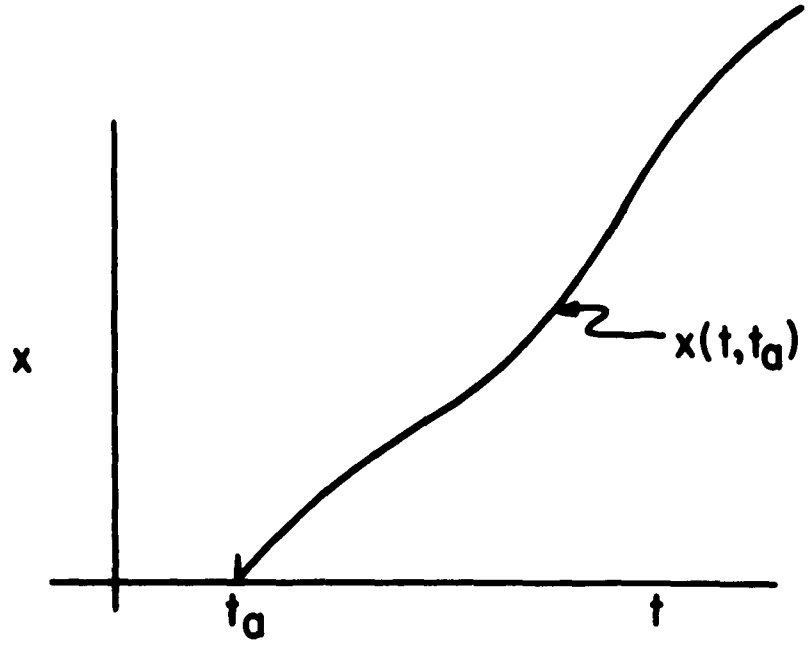

Figure 1

velocity v_o. The implication is that each element of the fluid is performing simple harmonic motion at the radian frequency ω_p independent of the amplitude of excitation, in addition to its drift at velocity v_o. Thus, a model of selected elements or discrete particles, which is chosen to approximate the continuous fluid model, should show similar motion.

The one-dimensional model to be used here, consists of electrons in a neutralizing background of positive charges. One choice is to let the fluid of electrons and the ions be represented as a manageable number of discrete particles, that is, as negatively and positively charged sheets. The sheets may be thought of as locations of point charges of very low density and, therefore, may oscillate through one another. Starting from near uniformity (i.e., + and - sheets interlaced and equally spaced from each other), with initial displacements less than the sheet spacing there will be no motion; this is unlike a plasma. Starting with initial velocities just large enough to cause nearest-neighbor-crossovers, the motion will be oscillatory, to be sure, but is <u>not</u> simple harmonic (not sinusoidal, but anharmonic) and the period is dependent on the amplitude of excitation. In order to make the electron sheets perform simple harmonic motion, as in the fluid model, each electron sheet must be given sufficiently large excitation to cross over many ion sheets in a period. For trajectory calculations, accounting for the crossovers is a bit messy because the force jumps at each crossover. However, note that real ions are much heavier than real electrons ($m_i/m_e \geq 1836$) so that ion motion is generally very small compared with electron motion, so small that it will be neglected here. Hence, the ion motion is "solved" and the ions no longer need to be made discrete but can be left as a uniform fluid or background. In this model, the electron sheets, even for the smallest excitation will cross over ions, and execute simple harmonic motion. The remaining restriction in the present calculation is that the electron sheets are driven weakly so that they do not cross each other, which is equivalent to the requirement of a single-valued

electron velocity in the fluid model. (Large drive will cause electron crossovers, making a direct solution difficult, but easily handled on a high-speed computer.)

The model to be analyzed is sketched in Figure 2. A portion of a typical charge density and electric field pattern is shown in Figure 3, assuming electron sheets of finite thickness.

The detailed motion is found readily from the isolated electron-sheet, ion-block pair shown in Figure 4. The total charge is assumed to be zero, so that

$$-\rho_e d_e = \rho_i d_i \tag{2}$$

The ion block has been assumed to be incompressible; d_i is constant. The electron sheet also is considered incompressible so that it moves under the influence of the force spatially averaged over the sheet. The center of the sheet sees average field $\overline{E}$ as shown, given by

$$\overline{E} = \frac{\rho_i}{\epsilon_o}(x - x_o) \qquad \left| x - x_o \right| \leq \frac{d_i + d_e}{2} \tag{3}$$

Because the field, hence force, is proportional to displacement, it is derivable from a potential which is parabolic, $V \sim (x - x_o)^2$. In the equation of motion, the charge-to-mass ratio of the sheet appears; this is simply e/m of a single electron. Thus, this equation is

$$\frac{\partial^2 x}{\partial t^2} = \left(\frac{e}{m}\frac{\rho_i}{\epsilon_o}\right)(x - x_o) = -\omega_p^2 (x - x_o) \tag{4}$$

This is the equation of simple harmonic motion, as desired. The plasma frequency used here is defined by

$$\omega_p^2 \equiv -\frac{e}{m}\frac{\rho_i}{\epsilon_o} \tag{5}$$

using the electron charge and mass but the ion background density; the sheet and block thicknesses do not appear explicitly and may be made arbitrarily large or small, e. g. , $d_e \rightarrow 0$

Lastly, many pairs may be placed one after the other, making the background continuous and uniform for equal ρ_i's The x_o's will be taken

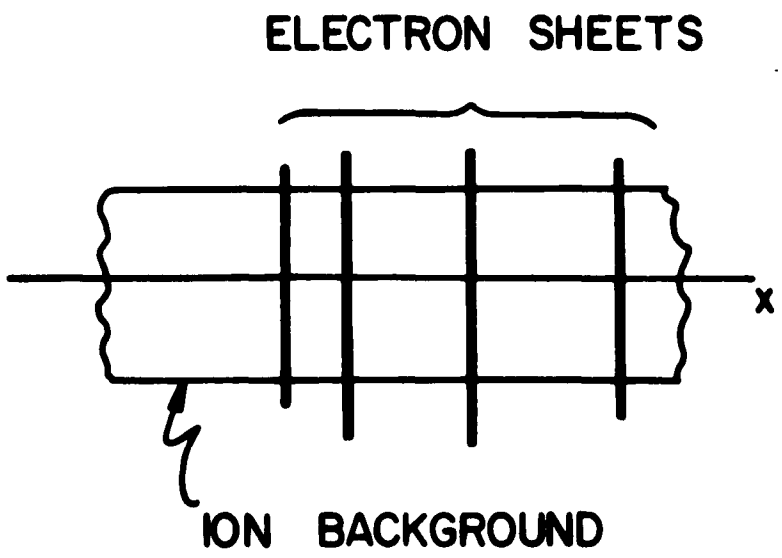

Figure 2

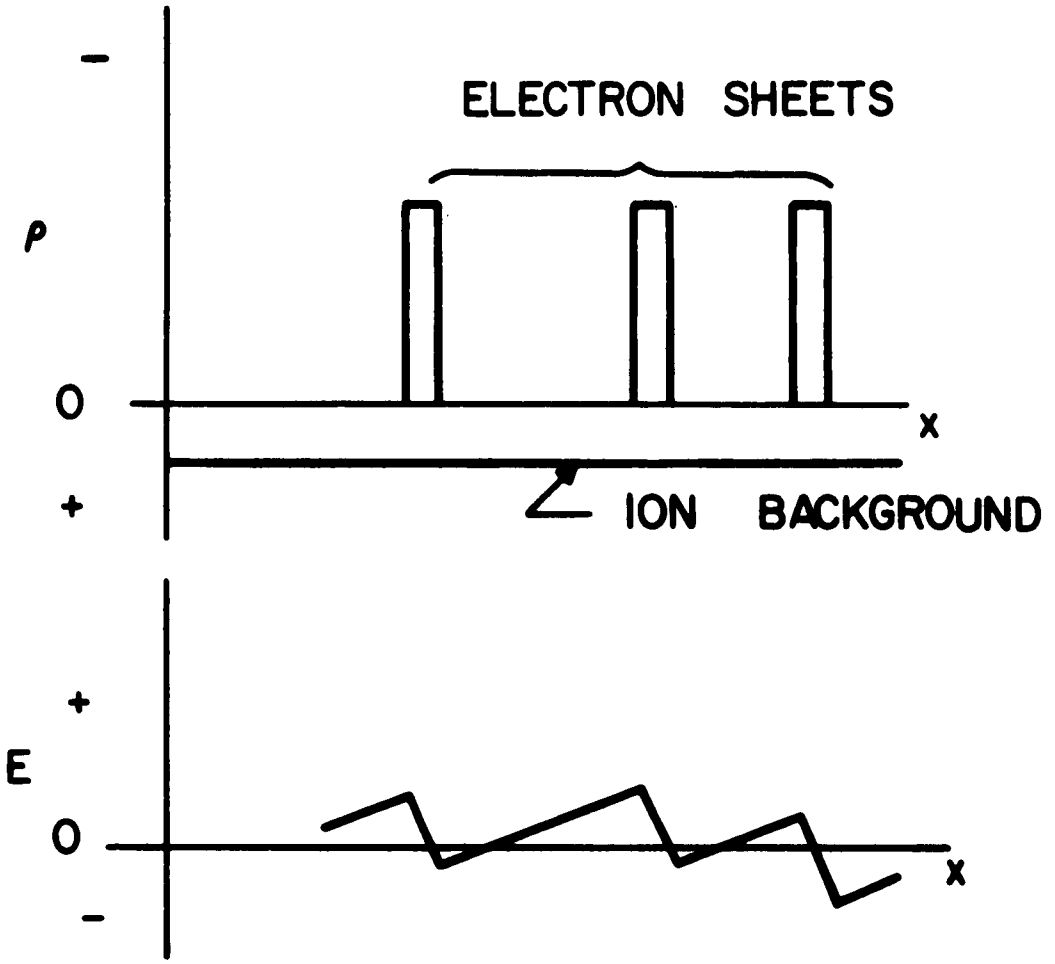

Figure 3

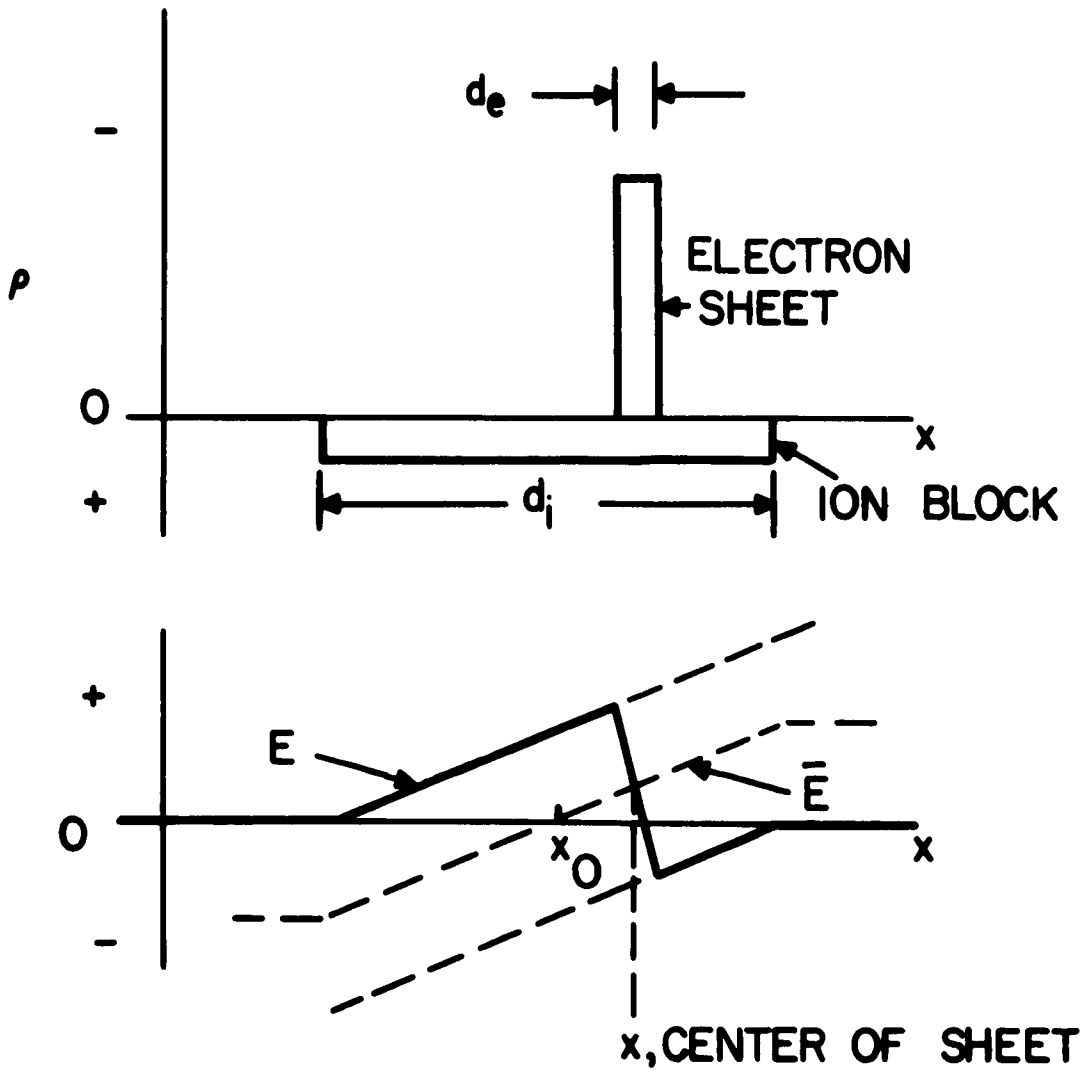
d_e
−
ELECTRON
SHEET
ρ
0
x
+
d_i
ION BLOCK
+
E
$\bar{E}$
0
x_0
x
−
x, CENTER OF SHEET

Figure 4

arbitrarily as the center of each block, an obvious equilibrium point, so that the above equation of motion still holds. However, with the background now continuous, any sheet may leave its parent block; the only restriction imposed in this study is that sheets may not cross each other. Thus, the notion of blocks may be set aside, and one need keep track of only the sheet and the equilibrium positions.

The block-sheet model may be extended to other symmetries. Starting with a uniform quiescent sea of electrons and (immobile) ions and making a local displacement of electrons along one coordinate r, one can readily obtain the equation of motion. Let the equilibrium radius be r_o and the displaced electron shell be at $r = r_o (1 + \delta)$. Then the electron motion is governed by

$$\frac{\partial^2 \delta}{\partial t^2} \doteq - \frac{\omega_p^2}{n+1} \left[\frac{(1 + \delta)^{n+1} - 1}{(1 + \delta)^n} \right] \tag{6}$$

$n = 0, 1, 2$ for planar, cylindrical and spherical displacements, respectively. The motion will be oscillatory but not, in general, simple harmonic. For all planar displacements ($n = 0$) but only for small cylindrical and spherical displacements ($n = 1, 2, \delta \ll 1$) this equation reduces to

$$\frac{\partial^2 \delta}{\partial t^2} \cong - \omega_p^2 \delta \tag{7}$$

Thus, simple harmonic motion is obtained only under these restrictions. See Dawson (1959) and Jackson (1960).

PARTICLE DISPLACEMENT

Particle orbits are obtained by integrating the equation of motion of each particle. The general answer, for the a^{th} particle is

$$x = x(t, t_a) \tag{1}$$

$$= x_o + F(t_a) \cos \omega_p (t - t_a) + G(t_a) \sin \omega_p (t - t_a) \tag{2}$$

The F's and G's are the two independent constants allowed by the second order equation of motion; they may be arbitrary functions of t_a. A similar equation will hold for the b^{th}, c^{th} . . . particles, each with its own x_o, F and G. The displacement of each particle is independent of the others so long as there are no crossings, i.e., the order of the sheets is maintained. If two sheets do cross, they must exchange x_o's, making a jump in the force; velocity and displacement are continuous through the crossover.

DRIFT VELOCITY

Each particle executes simple harmonic motion about its equilibrium position, x_o. It is desirable to obtain the motion of particles in a drifting stream from these results. Hence, the equilibrium positions will be made to drift at velocity v_o, that is,

$$x_o = v_o (t - t_{oa}) \tag{1}$$

Or, the original frame of observation may be considered to be drifting at velocity v_o so that a simple (Galilean) transformation may be made to the laboratory frame to obtain the drift-plus-oscillatory motion. t_{oa} is the departure time of the observer's frame for the a^{th} electron and is different from t_a if there is an initial displacement. On occasion, it may be inconvenient to carry t_{oa}, a fictitious departure time and hence, it is desirable to have a way to eliminate t_{oa}. Using $x = 0$ at $t = t_a$, the displacement equation is

$$0 = v_o(t_a - t_{oa}) + F(t_a). \tag{2}$$

From this result, one forms

$$x(t, t_a) = v_o(t - t_a) + F(t_a)\left[\cos \omega_p(t - t_a) - 1\right] + G(t_a)\left[\sin \omega_p(t - t_a)\right] \tag{3}$$

The pertinent times are shown in Figure 5.

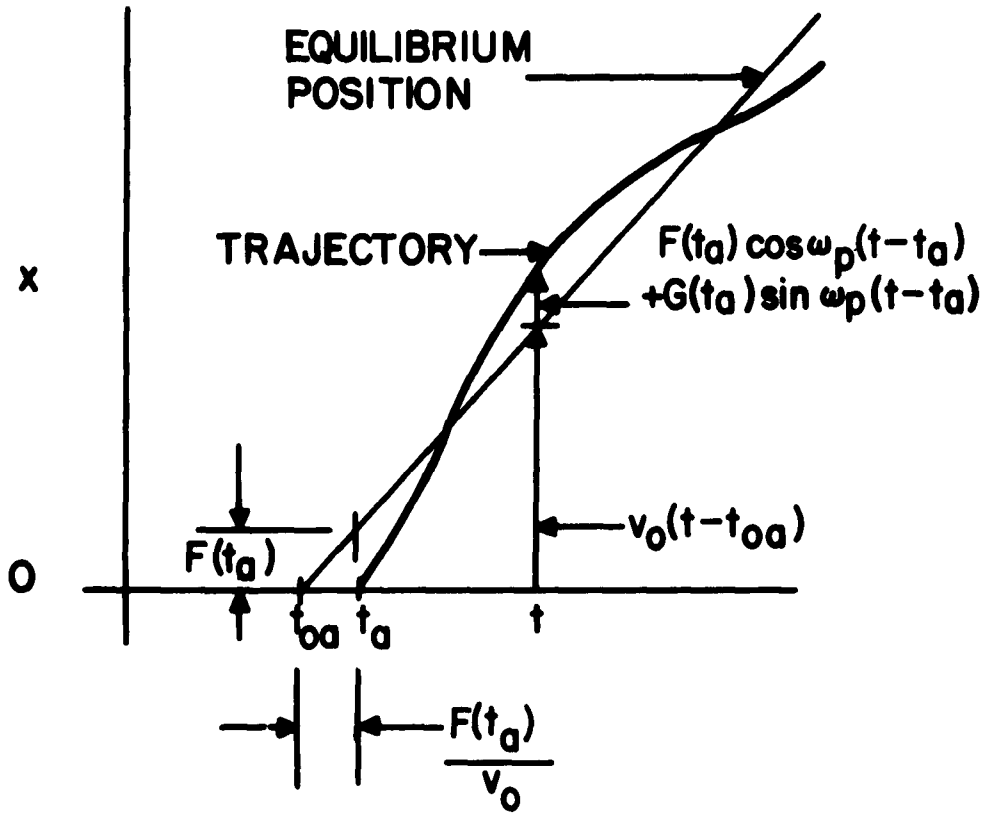
EQUILIBRIUM
POSITION
TRAJECTORY
x
O
F(t_a) cos ω_p(t−t_a)
+G(t_a) sin ω_p(t−t_a)
v_o(t−t_oa)
F(t_a)
t_oa
t_a
t
F(t_a)
v_o

Figure 5

One might ask whether t_{oa} and v_o vary with t_a; that is, may the ion blocks depart at arbitrary times with arbitrary velocity? In general, the answer is yes, but this would mean letting the background vary. In the restricted uses here, the answer is no. The individuality of the blocks is to be suppressed and the background charge density is to remain a constant. Thus all blocks are alike, departing uniformly in time and with the same v_o. However, as $F(t_a)$ and $G(t_a)$ are not restricted, one is still quite free to put in arbitrary excitation of the electrons including steps, ramps etc., as well as periodic functions.

INITIAL VELOCITY

The constants F and G may be determined in several ways. Here, the choice is to specify two independent qualities at the input plane, the ac velocity and ac current density. The velocity of the a^{th} particle is

$$v(t,\ t_a) = \frac{\partial x}{\partial t} = v_o - F(t_a)\omega_p \sin \omega_p(t - t_a) + G(t_a)\omega_p \cos \omega_p(t - t_a) \qquad (1)$$

At the input, $x = 0$, $t = t_a$, the velocity is given by a constant value plus a time-dependent part,

$$v(t_a,\ t_a) = v_o + v_1(t_a) \qquad (2)$$

(The constant value, v_o, is the same as that of the equilibrium positions but is not necessarily the average value in the presence of modulation.) Hence,

$$v_1(t_a) = G(t_a)\omega_p \qquad (3)$$

determining one of the constants. Note that $v_1(t_a)$ may be quite arbitrary, periodic or otherwise.

INITIAL CURRENT DENSITY

The current density or particle flux depends on the rate of passage of electrons through an area; here the current density is simply proportional to the density of trajectories at a fixed x. Similarly, the charge density is proportional to the density of trajectories at a fixed t. Hence, if the problems "start" at a fixed plane, as occurs here, the obvious second initial condition to be specified is the current; however, for a problem starting at a given time, specifying charge density would be more fitting.

The calculation current density can be made with the aid of Figure 6, showing two adjacent trajectories. The direct or steady current density, i_o, is inversely proportional to $t_{ob} - t_{oa}$, or

$$i_o = \frac{\rho_s}{t_{ob} - t_{oa}} \tag{1}$$

ρ_s is the charge / area of the electron sheet, $\rho_e d_e$, and is a negative number. The total current density depends on the actual time between sheets, which is, at x = 0, using Eq. (2) under Drift Velocity,

$$t_b - t_a = (t_{ob} - t_{oa}) - \left[\frac{F(t_b)}{v_o} - \frac{F(t_a)}{v_o}\right] \tag{2}$$

As $F(t_a)$ is a continuous function in the limit, it may be expanded as

$$F(t_b) = F(t_a) + \frac{dF(t_a)}{dt_a}(t_b - t_a) + - - - \tag{3}$$

Putting this into (2) and solving for $t_b - t_a$, one obtains

$$t_b - t_a = (t_{ob} - t_{oa})\left[1 + \frac{1}{v_o}\frac{dF(t_a)}{dt_a}\right]^{-1} \tag{4}$$

Hence, the current density at x = 0 is

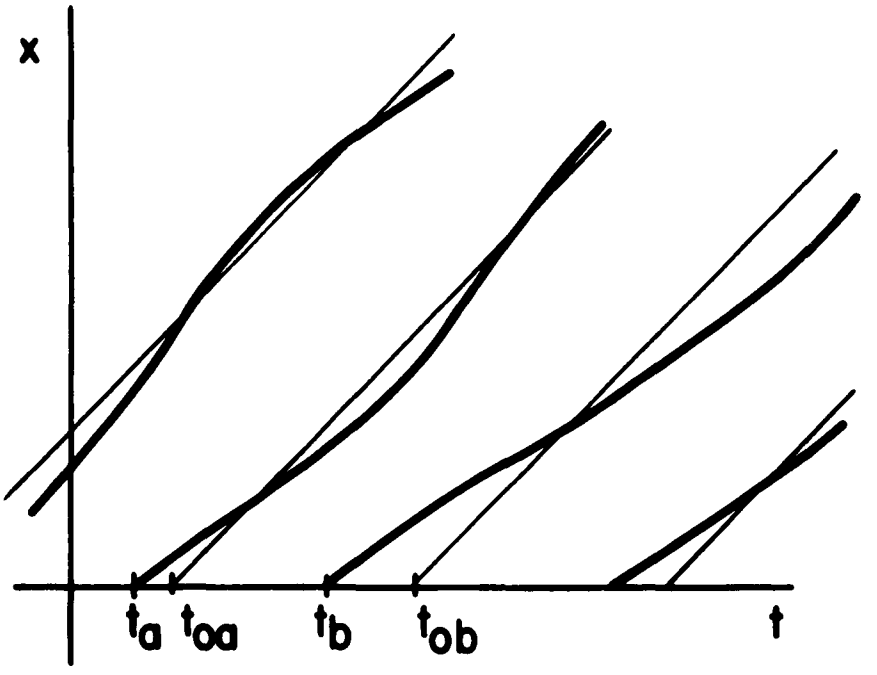

Figure 6

$$i(t_a, t_a) = \lim_{t_b \to t_a} \left(\frac{\rho_s}{t_b - t_a} \right) \tag{5}$$

$$= i_o \left[1 + \frac{1}{v_o} \frac{dF(t_a)}{dt_a} \right] \tag{6}$$

At the input, $x = 0$, $t = t_a$, the current density is given by a constant value plus a time-dependent part,

$$i(t_a, t_a) = i_o + i_1(t_a) \tag{7}$$

(The constant value, i_o, is the current density for no modulation but is not necessarily the average value in the presence of modulation.) Thus, one has,

$$i_1(t_a) = \frac{i_o}{v_o} \frac{dF(t_a)}{dt_a} \tag{8}$$

Thus (4) becomes simply,

$$t_b - t_a = (t_{ob} - t_{oa}) \left[1 + \frac{i_1(t_a)}{i_o} \right]^{-1} \tag{9}$$

Integrating (8), $F(t_a)$ is given by,

$$F(t_a) = \frac{v_o}{i_o} \int_{t_o}^{t_a} i_1(t_a)\, dt_a \tag{10}$$

The integral is made definite by saying that for $t_a < t_o$ there is no current modulation, and hence, no displacement from uniformity; the current modulation, periodic or otherwise starts at $t_a = t_o$. Thus $F(t_a)$ is an accumulated shift from no modulation. Physically, $i_1 dt_a$ is the ac charge density added or taken away from the unmodulated flow and the integral is the accumulated charge added or taken away. In the usual case of a periodic input current, $i_1(t_a)$, of course, may be given by a Fourier series, with a typical term $i_n \cos n\omega t_a$; then $F'(t_a)$ must have the same term, and $F(t_a)$ must have the term

$$\frac{v_o}{i_o} \cdot \frac{i_n}{n\omega} \sin n\omega t_a$$

and the transient associated with the start of modulation at t_o generally can be neglected.

Starting from fundamentals, not using the preceding results, one may show that the initial ac charge density is given by

$$\rho_1 (t_a, t_a) = \frac{\rho_o}{v_o} \left[\frac{dF(t_a)}{dt_a} - \omega_p G(t_a) \right]$$

The current at any plane, $i(t, t_a)$, may be found in terms of $F(t_a)$, $G(t_a)$ and $(t-t_a)$. The interested reader is advised to start from a statement of conservation of charge,

$$i(t_a, t_a)\ dt_a = i(t, t_a)\ dt.$$

LIMITS ON EXCITATION

In the cases of interest here, the excitation is to be maintained sufficiently small so that sheets do not cross over, that is, the ordering of sheets is to remain fixed. At a fixed x, going to larger t, one must find sheets that departed later, that is

$$\left. \frac{\partial t_a}{\partial t} \right|_x > 0 \qquad (1)$$

This ratio may be calculated from

$$\left. \frac{\partial t_a}{\partial t} \right|_x = - \frac{\partial x / \partial t}{\partial x / \partial t_a}$$

Or, at a fixed t, going to larger x, one must find sheets that left earlier, that is

$$\left. \frac{\partial x}{\partial t_a} \right|_t < 0 \qquad (2)$$

Or, in a problem, which starts at a fixed time, $t = 0$ with electrons initially ordered as x_a, x_b etc.; ordering is maintained at a later time if

$$\left.\frac{\partial x}{\partial x_a}\right|_t > 0 \qquad (3)$$

(In this problem $t - t_a$ is replaced by $t - 0 = t$ and $F(t_a)$, $G(t_a)$ are replaced by $F(x_a)$, $G(x_a)$. At crossings, the densities become infinite.

As brought out in the examples to follow, the excitations can be quite large before overtaking occurs, considerably larger than allowed in the small-signal Eulerian fluid analysis where higher order terms are dropped, and no harmonics are allowed. Here, no such restrictions occur. The only problem is with overtaking and that could be obviated by renumbering.

Example (1). Assuming a velocity modulation of

$$v_1(t_a) = v_1 \cos \omega t_a$$

crossing just occurs for $\omega > \omega_p$ with

$$\frac{v_1}{v_o} = \frac{\omega_p}{\omega},$$

between the electrons that left in the vicinity of $\omega t_a \sim -\pi/2$ (or $3\pi/2$, etc.) at $\omega_p(t-t_a) = \pi/2$, one quarter plasma cycle after modulation. For $\omega < \omega_p$, $v_1/v_o \geq 1$ causes crossings at the input between electrons near $\omega t_a = -\pi$. Thus, one may plot the maximum allowable velocity modulation as in Figure 7a.

Example (2). Assuming a current modulation of

$$i_1(t_a) = i_1 \cos(\omega t_a - \phi)$$

crossing just occurs for $\omega > \frac{\omega_p}{2}$ at

$$\frac{i_1}{i_o} = 0.5$$

between the electrons leaving near $(\omega t_a - \phi) \cong \pi$ at the input. For $\omega < \frac{\omega_p}{2}$ crossing just occurs for

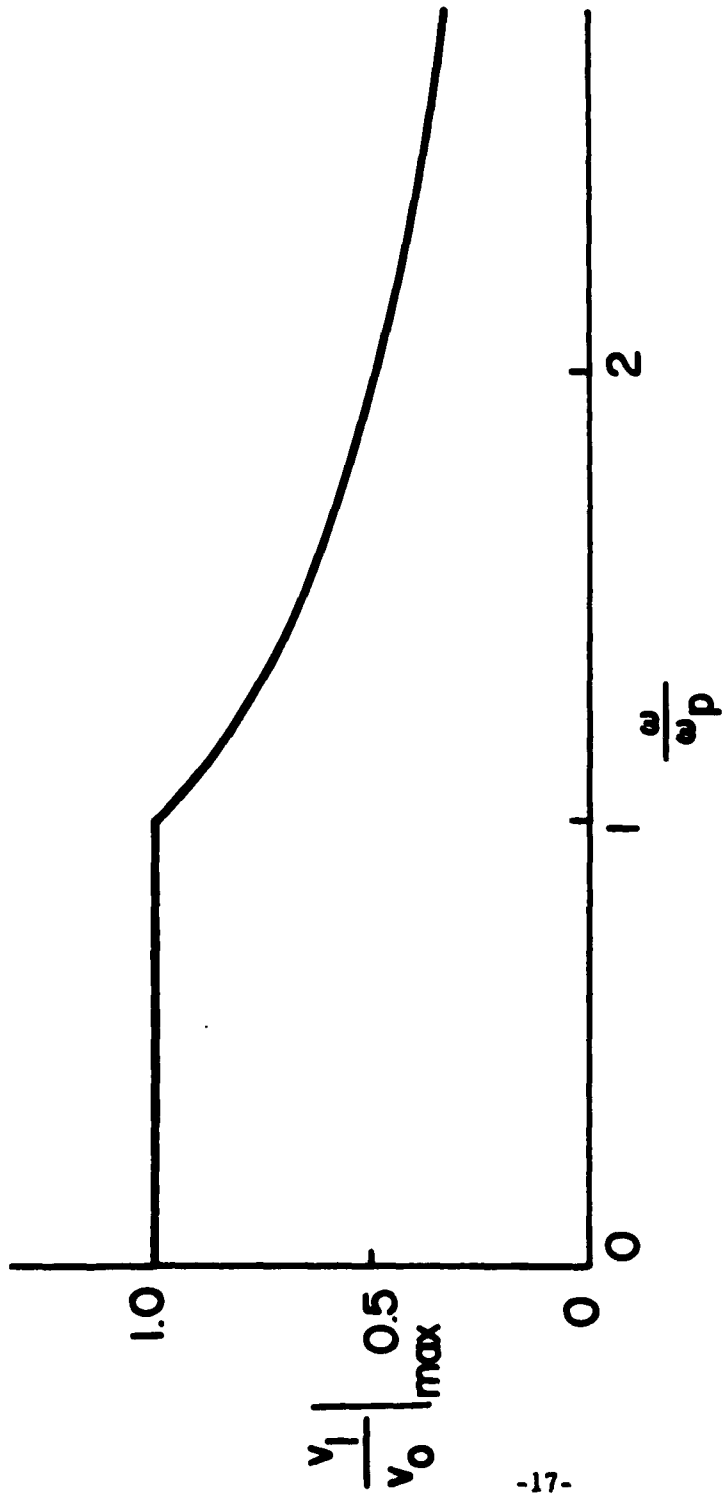

Figure 7a

$$\frac{i_1}{i_o} \equiv \frac{\omega}{\omega_p}$$

for crossings between $(\omega t_a - \phi) \cong + \pi/2$ electrons at $\omega_p(t - t_a) = \pi/2$ one quarter plasma cycle after modulation. These results are shown in Figure 7b.

Example (3). For excitation of the slower space-charge wave only, the limits of excitation in velocity and current are

$$\frac{v_1}{v_o} \ll 1/(1 + \frac{2\omega}{\omega_p}); \quad \frac{i_1}{i_o} < (\omega/\omega_p) \Big/ (1 + \frac{2\omega}{\omega_p})$$

as shown in Figure 7c.

Example (4). For excitation of the faster-wave only for $\omega \ll \omega_p$

$$\frac{v_1}{v_o} < 1, \frac{i_1}{i_o} \quad \frac{\omega}{\omega_p}$$

and for $\omega > \omega_p$

$$\frac{v_1}{v_o} < 1/(-1 + \frac{2\omega}{\omega_p}); \quad \frac{i_1}{i_o} < (\omega/\omega_p) \; / \; (-1 + \frac{2\omega}{\omega_p})$$

as shown in Figure 7d.

RELATION TO FLUID MODEL

The particle results may be put in the form that goes with the continuous fluid model used in the original space-charge wave work of Hahn and Ramo (1939). In the present form, one has the particle position $x(t, t_a)$; in the fluid model, the dependent variables are given, for example, as $v(x, t)$. The transformation from one system to the other is obtained by going to a frame moving at velocity v_o, as was mentioned earlier, and observing the streaming.

An observer leaves $x = 0$ at $t = t_{oa}$ with velocity v_o and has position

$$x = v_o(t - t_{oa}) \tag{1}$$

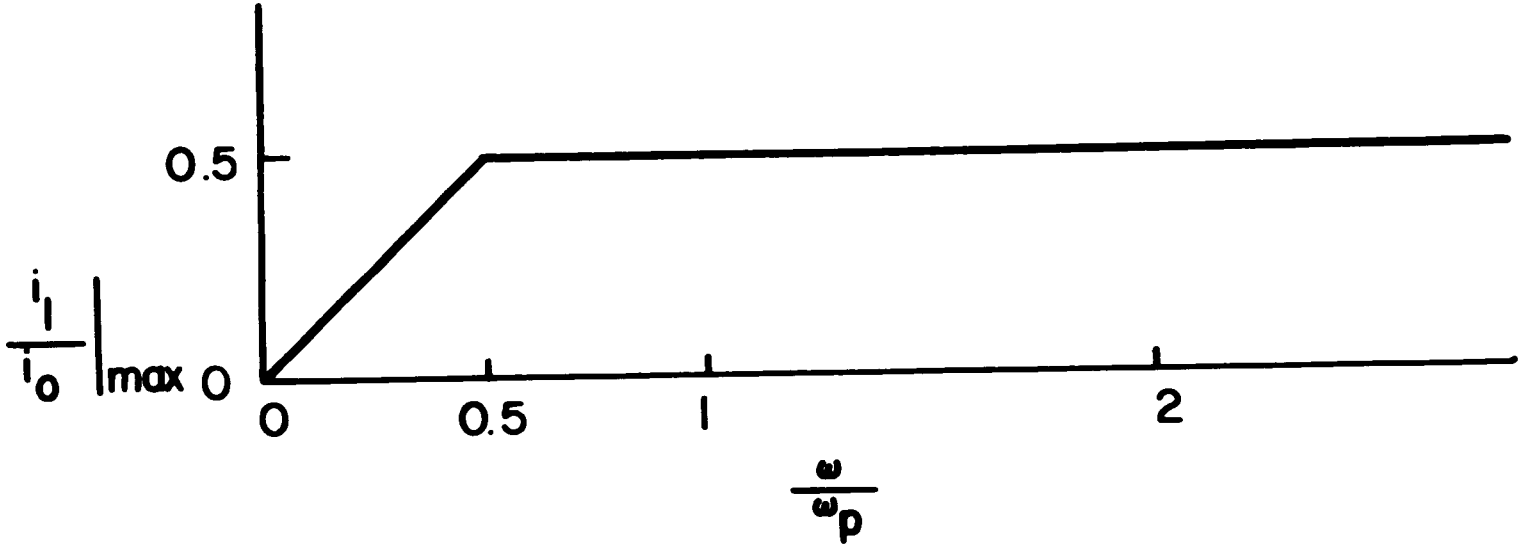

Figure 7b

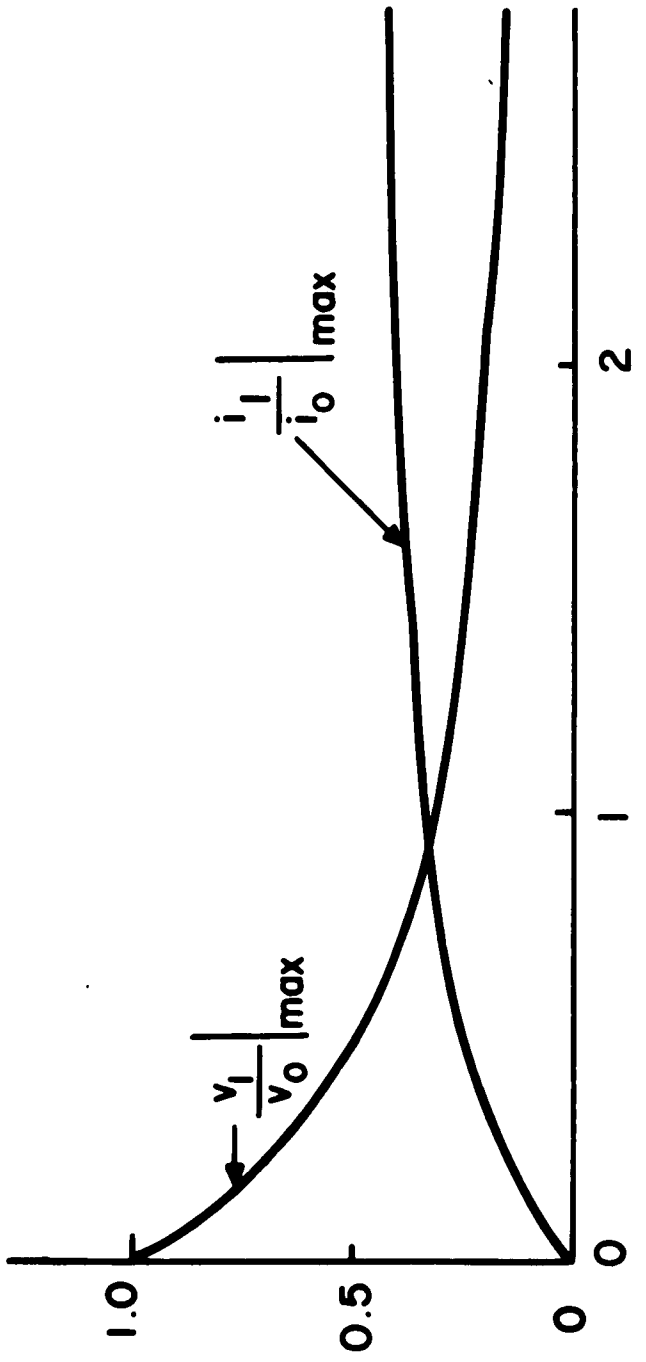
1.0
0.5
0
0
1
2
$\frac{\omega}{\omega_p}$
$\left|\frac{v_1}{v_o}\right|_{max}$
$\left|\frac{i_1}{i_o}\right|_{max}$

Figure 7c

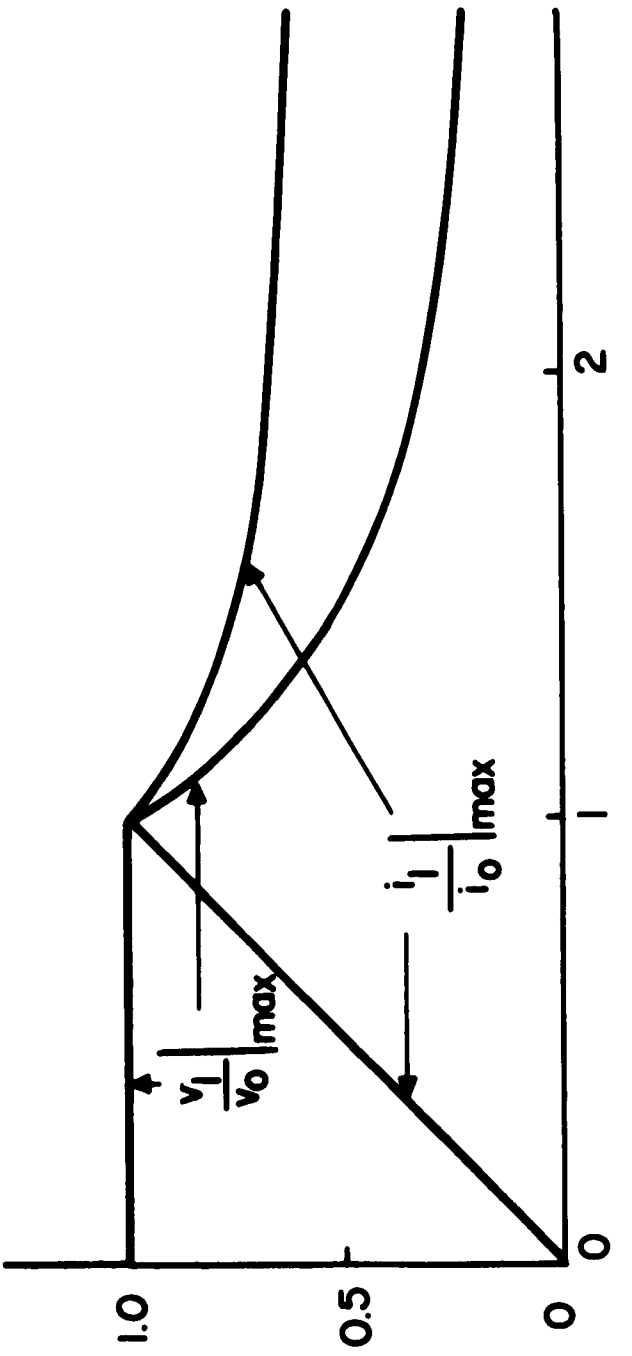
1.0
0.5
0
0
1
2
$\frac{\omega}{\omega_p}$
$\left|\frac{v_1}{v_0}\right|_{max}$
$\left|\frac{i_1}{i_0}\right|_{max}$

Figure 7d

Or, he measures time by

$$t = t_{oa} + \frac{x}{v_o} \tag{2}$$

$$= t_a + \frac{x + F(t_a)}{v_o} \tag{3}$$

The independent variable t_a may now be replaced in terms of t and x in the particle results,

$$F(t_a) \rightarrow F\left[t - \frac{x + F(t_a)}{v_o}\right] \tag{4}$$

or

$$\sin\ \omega_p (t - t_a) \rightarrow \sin\left[\frac{\omega_p}{v_o}\left(x + F(t_a)\right)\right] \tag{5}$$

However, the trigonometric terms multiply ac (first-order) terms, so that in the limit of very small current modulation, the ac term $F(t_a)$ in the arguments may be dropped. Hence, the ac displacement, as seen by the observer, is

$$x_1 = x_1\ (x,\ t) \tag{6}$$

$$= F\left(t - \frac{x}{v_o}\right)\ \cos\ \frac{\omega_p x}{v_o} + G\left(t - \frac{x}{v_o}\right)\ \sin\ \frac{\omega_p x}{v_o} \tag{7}$$

The wavelike nature, which was completely suppressed in the particle picture, is once more evident. However, here one treats x and t as independent variables, no longer connected together, as would be so for the trajectory of a given particle. The ac velocity, as seen by the observer, is obtained from

$$v_1 = v_1\ (x,\ t) \tag{8}$$

$$= \frac{dx_1}{dt} \tag{9}$$

$$= \frac{\partial x_1}{\partial t} + v_o \frac{\partial x_1}{\partial x} \tag{10}$$

F and G are functions of a single variable so that one may write

$$\frac{\partial F}{\partial t} = F', \qquad \frac{\partial F}{\partial x} = - \frac{1}{v_o} F' \tag{11}$$

Thus

$$v_1 (x, t) = \omega_p G (t - \frac{x}{v_o}) \cos \frac{\omega_p x}{v_o} - \omega_p F (t - \frac{x}{v_o}) \sin \frac{\omega_p x}{v_o} \tag{12}$$

At $x = 0$, let

$$v_1 (0, t) = v_1 \cos \omega t \tag{13}$$

$$= \omega_p G (t - \frac{0}{v_o}) \tag{14}$$

or

$$G (t - \frac{x}{v_o}) = v_1 \cos \omega \left(t - \frac{x}{v_o}\right) \tag{15}$$

The current density $i_1 (x, t)$ must obey

$$i_1 (x, t) = - \epsilon_o \frac{\partial E_1}{\partial t} \tag{16}$$

E_1 was obtained earlier as

$$E_1 = \frac{\rho_i}{\epsilon_o} (x - x_o) \tag{17}$$

$$= \frac{\rho_i}{\epsilon_o} x_1$$

$$= - \frac{\rho_o}{\epsilon_o} x_1$$

(The ion charge density, ρ_i, is the negative of the electron charge density, ρ_o, in the fluid model.) Hence,

$$i_1(x,\ t) = \rho_o \frac{\partial x_1}{\partial t} \tag{18}$$

$$= \rho_o \left[F'\left(t - \frac{x}{v_o}\right) \cos \frac{\omega_p x}{v_o} + G'\ (t - \frac{x}{v_o}\ )\ \sin \frac{\omega_p x}{v_o} \right] \tag{19}$$

At $x = 0$, let

$$i_1(0,\ t) = i_1\ \cos\ (\omega t - \phi) \tag{20}$$

$$= \rho_o\ F'\ (t - \frac{0}{v_o}\ ) \tag{21}$$

or, integrating,

$$F\ (t - \frac{x}{v_o}\ ) = \frac{i_1}{\omega \rho_o}\ \sin\ (\omega t - \frac{x}{v_o} - \phi) \tag{22}$$

These results may be summarized, as

$$x_1(x,\ t) = \frac{i_1}{i_o}\ \frac{v_o}{\omega}\ \sin\ (\omega t - \frac{\omega x}{v_o} - \phi)\ \cos\ \frac{\omega_p x}{v_o} + \frac{v_1}{v_o}\ \frac{v_o}{\omega_p}\ \cos\ (\omega t - \frac{\omega x}{v_o})\ \sin \frac{\omega_p x}{v_o} \tag{23}$$

$$\frac{v_1}{v_o}\ (x,t) = \frac{v_1}{v_o}\ \cos\ (\omega t - \frac{\omega x}{v_o})\ \cos \frac{\omega_p x}{v_o} - \frac{i_1}{i_o}\ \frac{\omega_p}{\omega}\ \sin\ (\omega t - \frac{\omega x}{v_o} - \phi)\ \sin \frac{\omega_p x}{v_o} \tag{24}$$

$$\frac{i_1(x,t)}{i_o} = \frac{i_1}{i_o}\ \cos\ (\omega t - \frac{\omega x}{v_o} - \phi)\ \cos \frac{\omega_p x}{v_o} - \frac{v_1}{v_o}\ \frac{\omega}{\omega_p}\ \sin\ (\omega t - \frac{\omega x}{v_o}\ )\ \ \sin \frac{\omega_p x}{v_o} \tag{25}$$

ρ_1 may be obtained from

$$\rho_1(x,\ t) = \epsilon_o \frac{\partial E_1}{\partial x} \tag{26}$$

$$= -\rho_o \frac{\partial x_1}{\partial x} \tag{27}$$

The result is

$$\rho_1(x,\ t) = \frac{\rho_o}{v_o} \left[(F' - G\omega_p) \cos \frac{\omega_p x}{v_o} + (F\ \omega_p + G') \sin \frac{\omega_p x}{v_o} \right] \tag{28}$$

Hence

$$\frac{\rho_1(x,\ t)}{\rho_o} = \left[\frac{i_1}{i_o}\cos\left(\omega t - \frac{\omega x}{v_o} - \phi\right) - \frac{v_1}{v_o}\cos\left(\omega t - \frac{\omega x}{v_o}\right)\right]\cos\frac{\omega_p x}{v_o}$$

$$+\left[\frac{i_1}{i_o}\frac{\omega_p}{\omega}\sin\left(\omega t - \frac{\omega x}{v_o} - \phi\right) - \frac{v_1}{v_o}\frac{\omega}{\omega_p}\sin\left(\omega t - \frac{\omega x}{v_o}\right)\right]\sin\frac{\omega_p x}{v_o} \tag{29}$$

These results are the same as obtained for the fluid model.

One final word of caution; $x_1(x,\ t)$ as given here is the displacement from equilibrium of electrons as seen by an observer at $(x,\ t)$ and is <u>not</u> the displacement of a particular electron.

TRAJECTORY PLOTS

The properties of various kinds of modulation and of each wave may be made clearer using plots of electron trajectories. The method of obtaining these plots will be given in some detail for harmonic excitation. The starting point is with the displacement,

$$x(t,\ t_a) = v_o(t - t_{oa}) + F(t_a)\left[\cos\omega_p(t - t_a)\right] + G(t_a)\left[\sin\omega_p(t - t_a)\right]$$

The initial conditions are stated as

$$v_1(t_a) = v_1\cos\omega t_a \tag{1}$$

$$i_1(t_a) = i_1\cos(\omega t_a - \phi) \tag{2}$$

v_1 is real and positive and i_1 and i_o are real and negative. The displacement is

$$x(t,\ t_a) = v_o(t - t_{oa}) + \frac{i_1}{i_o}\frac{v_o}{\omega}\sin(\omega t_a - \phi)\cos\omega_p(t - t_a)$$

$$+\frac{v_1}{v_o}\frac{v_o}{\omega_p}\cos\omega t_a\sin\omega_p(t - t_a) \tag{3}$$

Or the $x_1(x, t)$ expression may be used with x and t properly related in the functions so as to follow a particular electron, i. e.,

$$x = v_o(t - t_{oa})$$

For plotting, one needs to have a schedule of departure times. These times occur uniformly in t_{oa}, but not in t_a. The electron departure times are

$$t_a = t_{oa} - \frac{1}{v_o} F(t_a) \tag{4}$$

$$= t_{oa} - \frac{i_1}{i_o} \frac{1}{\omega} \sin (\omega t_a - \phi) \tag{5}$$

This is a transcendental equation in t_a which can be solved numerically; for small current modulation, it can be solved approximately as,

$$t_a \cong t_{oa} - \frac{i_1}{i_o} \frac{1}{\omega} \sin (\omega t_{oa} - \phi) \tag{6}$$

The t_{oa}'s may be scheduled as

$$t_{oa} = t_{on} = n\Delta t \qquad n = 1, 2, 3 \ldots \tag{7}$$

where Δt is the uniform spacing, at a given x, of the ion blocks or equilibrium positions. For N electrons injected in each cycle, $\omega t = 2\pi$,

$$N \Delta t = 2 \pi \tag{8}$$

so

$$t_{on} = 2\pi \frac{n}{N} \tag{9}$$

Hence,

$$x (t, x_a) \longrightarrow x (t, n) \text{ or } x_n (t) \tag{10}$$

For convenience, the passage of time, $\omega_p (t - t_a)$, may be measured in terms of an equivalent distance. Let x_{on} be defined by

$$x_{on} = v_o (t - t_a) \Big|_{n^{th} \text{ electron}} \tag{11}$$

(This is the equilibrium position only in the case of no current modulation.) Then,

$$\omega_p(t-t_a) = \frac{\omega_p x_{on}}{v_o} \tag{12}$$

Hence $x(t, t_a)$ becomes $x(x_{on}, t_a)$

$$\frac{\omega_p x}{v_o}(x_{on}, t_a) = \omega_p(t - t_{oa}) + \frac{i_1}{i_o}\frac{\omega_p}{\omega}\sin(\omega t_a - \phi)\cos\left(\frac{\omega_p x_{on}}{v_o}\right) + \frac{v_1}{v_o}\cos\omega t_a \sin\left(\frac{\omega_p x_{on}}{v_o}\right) \tag{13}$$

In this form, trajectory plotting, x vs t, is straightforward:

By way of illustration, one may find the locus of turn-around points (where the ac velocity changes sign). For velocity modulation only, $t_a = t_{oa}$, and particles obey

$$x(t, t_a) = v_o(t - t_a) + \frac{v_1}{v_o}\frac{v_o}{\omega_p}\cos\omega t_a \sin\omega_p(t - t_a) \tag{14}$$

$$v(t, t_a) = v_o + v_1 \cos\omega t_a \cos\omega_p(t - t_a) \tag{15}$$

The maximum excursion from equilibrium occurs for $\omega_p(t - t_a) = \pi/2$ where the ac velocity vanishes, v is v_o; but the electron at turn around is not at

$$\frac{\omega_p x}{v_o} \text{ of } \pi/2, \text{ rather, at}$$

$$\left(\frac{\omega_p x}{v_o}\right) \text{ turn-around} = \frac{\pi}{2} + \frac{v_1}{v_o}\cos\omega t_a \tag{16}$$

This locus and some representative trajectories are shown in Figure 8.

SLOWER SPACE-CHARGE WAVE TRAJECTORIES

The slower space-charge wave by itself may be excited by proper choice of initial modulation. As known from space-charge wave analysis,

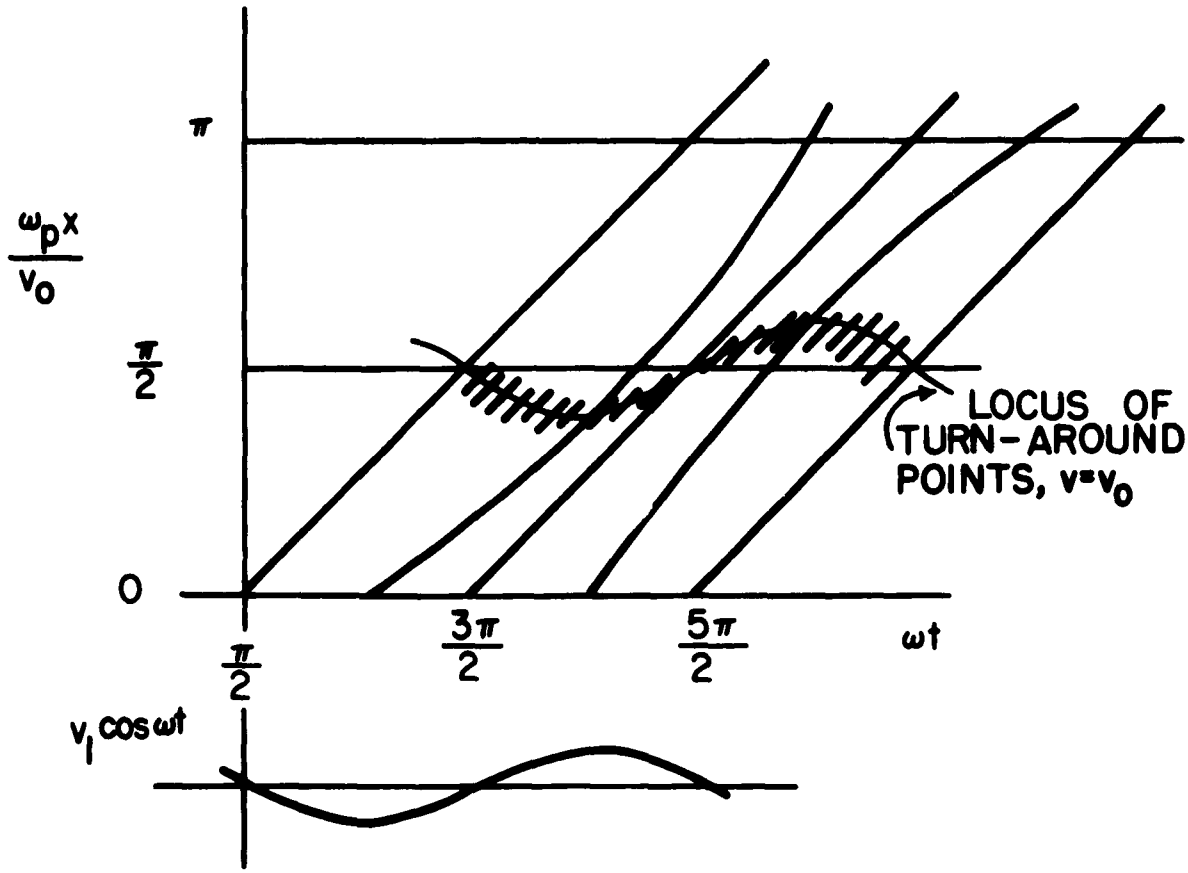
π
$\frac{\omega_p x}{v_0}$
$\frac{\pi}{2}$
0
$\frac{\pi}{2}$
$\frac{3\pi}{2}$
$\frac{5\pi}{2}$
ωt
LOCUS OF TURN-AROUND POINTS, v=v0
v1 cos ωt

Figure 8

this requires that the initial velocity and current modulation be π out of phase, $\phi = \pi$, and in the ratio

$$\frac{v_1}{v_o} = \frac{\omega_p}{\omega} \frac{i_1}{i_o} \tag{1}$$

Hence,

$$\frac{\omega_p}{v_o} x(t, t_a) = \omega_p (t - t_{oa}) - \frac{v_1}{v_o} \sin\left[\omega t_a - \omega_p (t - t_a)\right]$$

$$= \omega_p (t - t_{oa}) - \frac{v_1}{v_o} \sin\left[\omega t_a - \frac{\omega_p x_{on}}{v_o}\right] \tag{2}$$

Note that all all electrons have the same amplitude of oscillation.

Figures 9, 10, and 11 are plots of trajectories of the slower wave for ω/ω_p of 2, 1, 0.5. The regions of larger charge density are where the electrons are going slower, giving rise to negative ac kinetic energy density. The phase velocities for the figures are $2/3\ v_o$, $1/2\ v_o$ and $1/3\ v_o$, obviously corresponding to the velocities of propagation of the denser regions. The bunches are formed then reformed with electrons sliding <u>through</u> the bunches. There is no collection of particles which stays more or less together; that is, there is no trapping of particles.

FASTER SPACE-CHARGE WAVE TRAJECTORIES

Excitation of the faster space-charge wave by itself requires that the current and velocity modulation be in phase, $\phi = 0$ and in the ratio

$$\frac{v_1}{v_o} = \frac{\omega_p}{\omega} \frac{i_1}{i_o} \tag{1}$$

Hence,

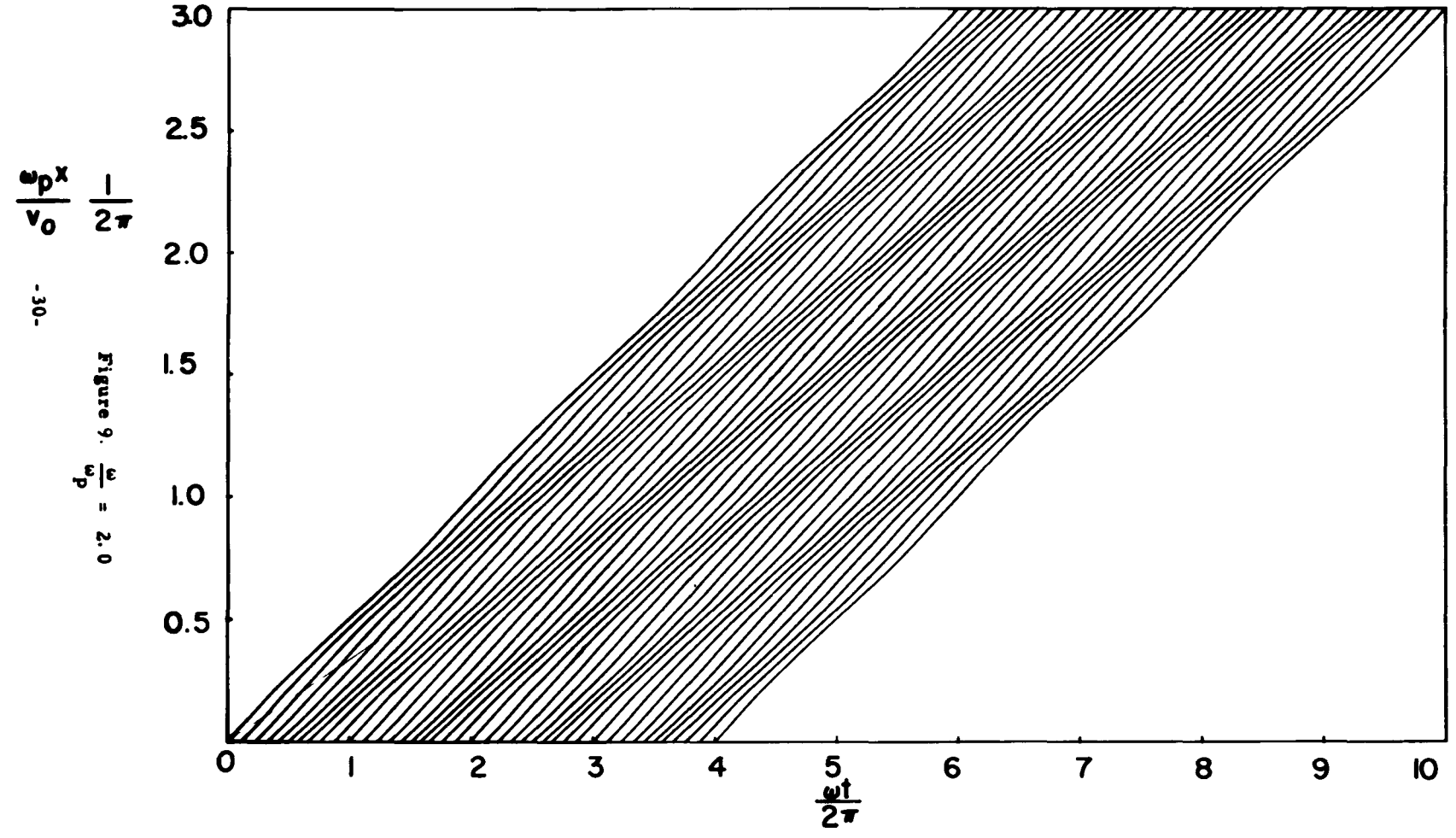

Figure 9. $\frac{\omega_p}{\omega} = 2.0$

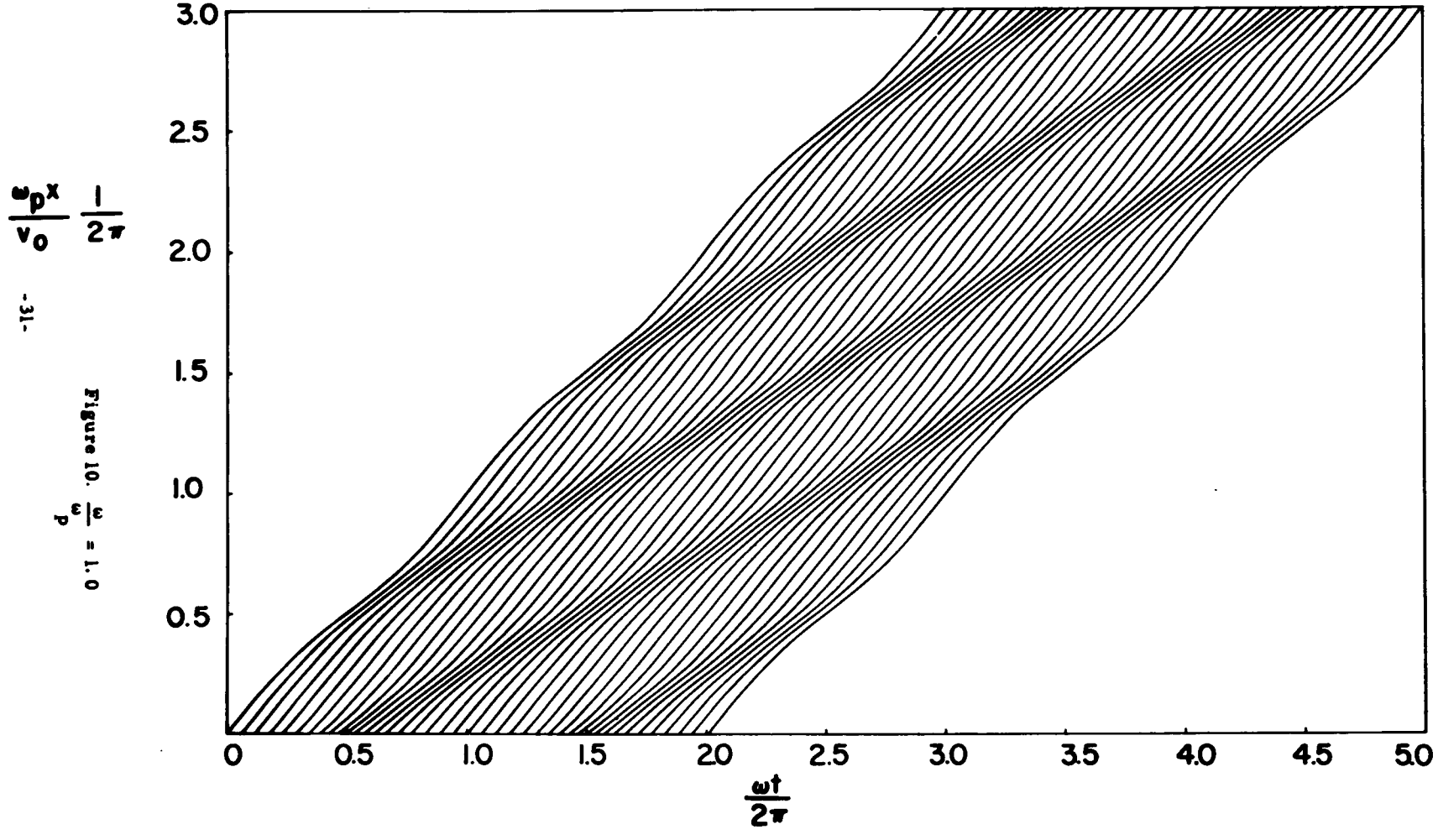

$\frac{\omega}{\omega_p} = 1.0$

Figure 10.

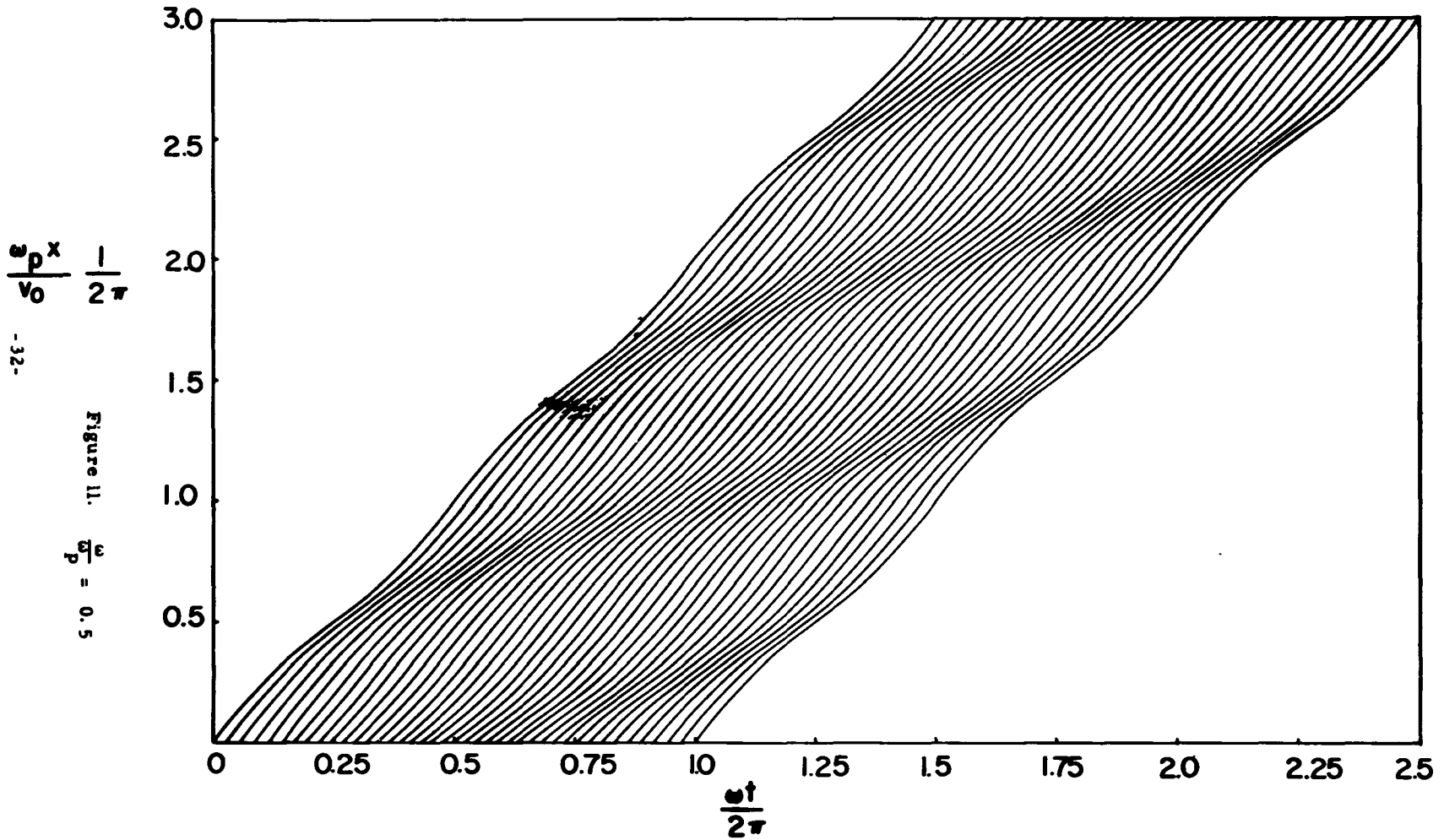

Figure 11. $\frac{\omega}{\omega_p} = 0.5$

$$\frac{\omega_p}{v_o} x(t, t_a) = \omega_p (t - t_{oa}) + \frac{v_1}{v_o} \sin\left[\omega t_a + \omega_p (t - t_a)\right]$$

$$= \omega_p (t - t_{oa}) + \frac{v_1}{v_o} \sin\left[\omega t_a + \frac{\omega_p x_{on}}{v_o}\right] \qquad (2)$$

Again, the amplitudes of oscillation are all the same. Figures 12, 13, 14 show the trajectories for $\omega/\omega_p = 2, 1, 0.5$. Here the regions of larger charge density occur where electrons are going faster, giving rise to positive kinetic energy density. The phase velocities are $2v_o$, ∞, and $-v_o$, not so obviously tied to the velocities of the denser regions as is true with the slower wave. For $\omega = \omega_p$, only i_{1f} and v_{1f} are excited and ρ_{1f} is zero; hence at fixed t, the spacings of the trajectories remain fixed. In addition, as $\rho_{1s} = 0$, $\partial E/\partial x = 0$, so $E_1 = E_1(t)$ independent of x; thus the electric field over all space is merely oscillating with time at $\omega = \omega_p$.

VELOCITY MODULATION, WAVE INTERFERENCE

For velocity modulation only, both waves are excited. The displacement is,

$$\frac{\omega_p}{v_o} x(t, t_a) = \omega_p (t - t_{oa}) + \frac{v_1}{v_o} \cos \omega t_a \sin \omega_p (t - t_a) \qquad (1)$$

Plots of these trajectories are given in Figures 15, 16, 17 for ω/ω_p of 2, 1.0, 0.5. Here the wave interference between the faster and slower waves is evident. The slower-wave tends to be predominant, due to absence of ρ_{1-} at $\omega = \omega_p$ and, in the other two plots, because $\left|\rho_{1+}\right| = 3\left|\rho_{1-}\right|$. v_{1+} and v_{1-} are equally excited as are i_{1+} and i_{1-} at all frequencies.

Although the current density is always a maximum at $\lambda_p/4$ from the plane of excitation, independent of ω/ω_p, the charge density follows the sine law only for large ω/ω_p. In the small ω/ω_p region, the charge density follows a cosine law and gives the appearance of strung out bunching, as seen in the figures.

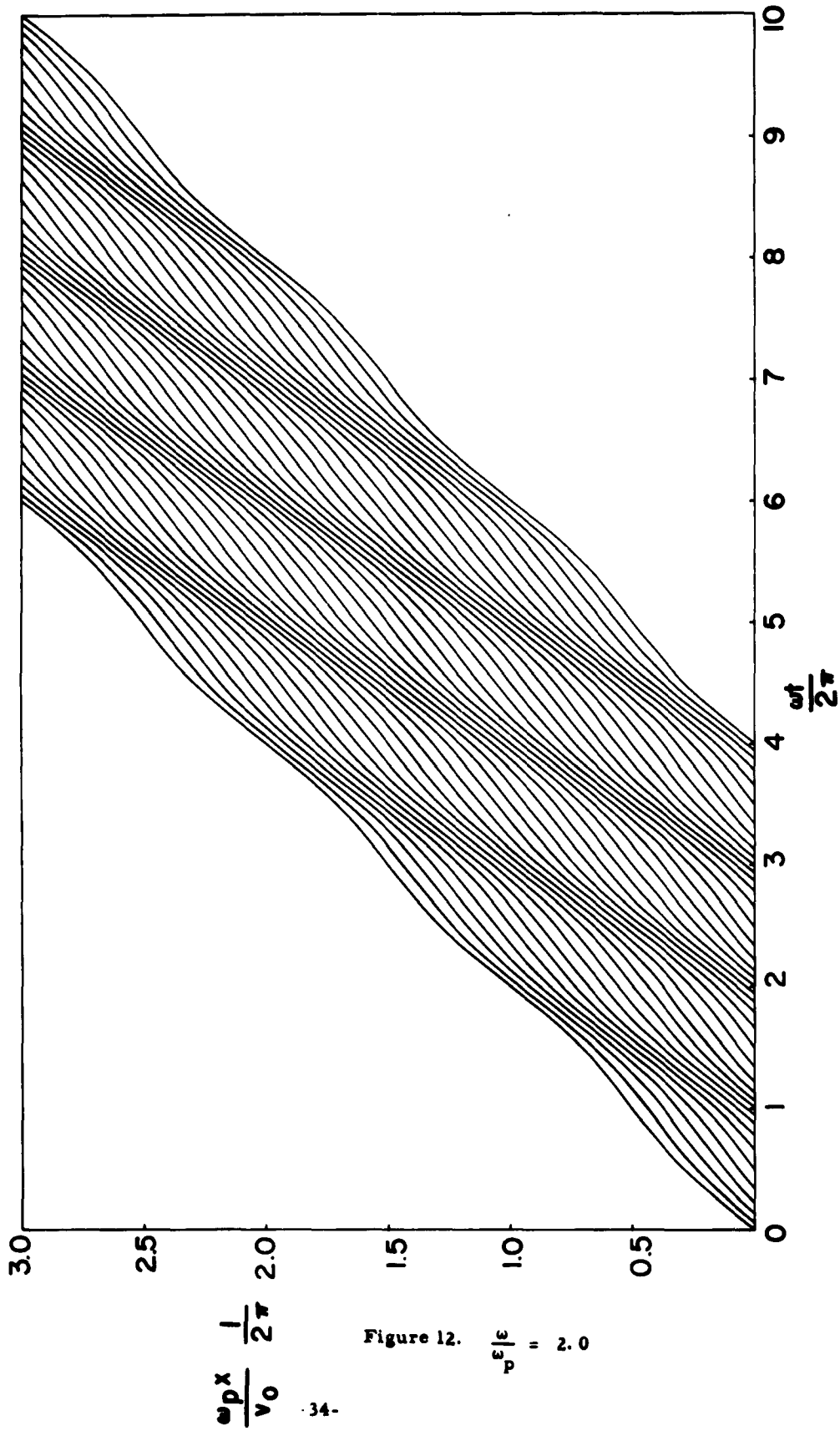

Figure 12. $\frac{\varepsilon}{\varepsilon_p} = 2.0$

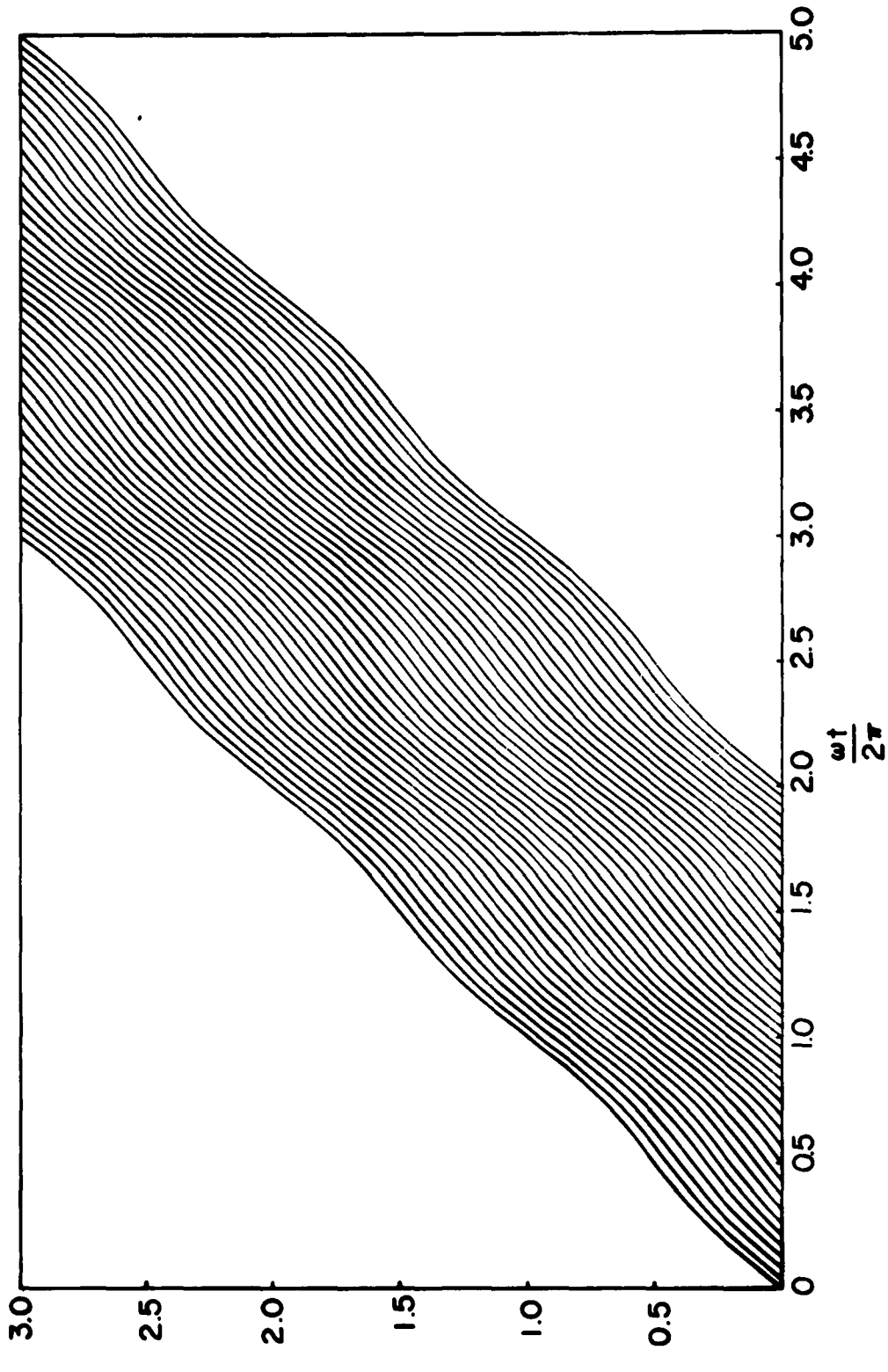

Figure 13. $\frac{\varepsilon}{\varepsilon_p} = 1.0$

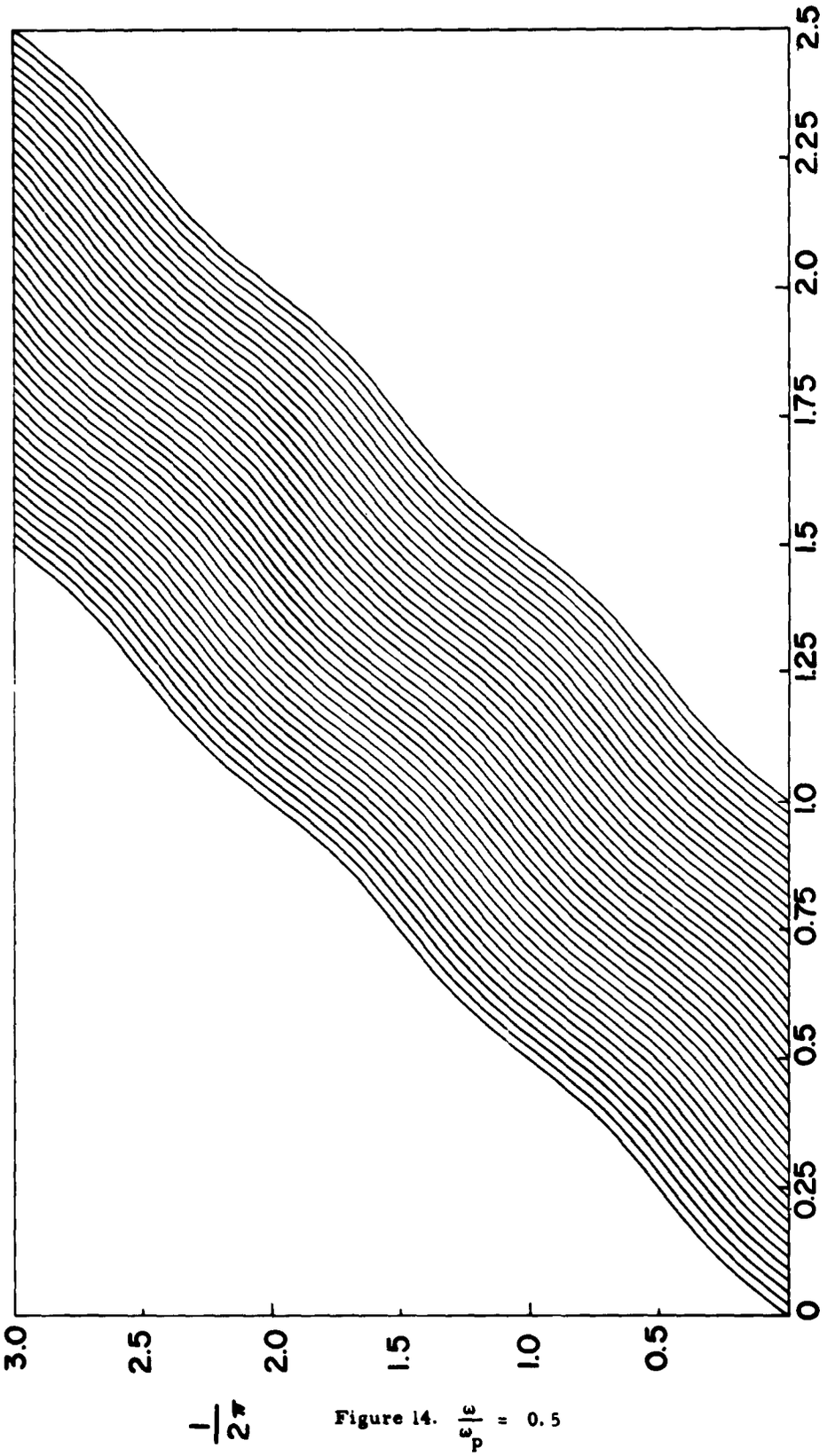

Figure 14. $\frac{\omega}{\omega_p} = 0.5$

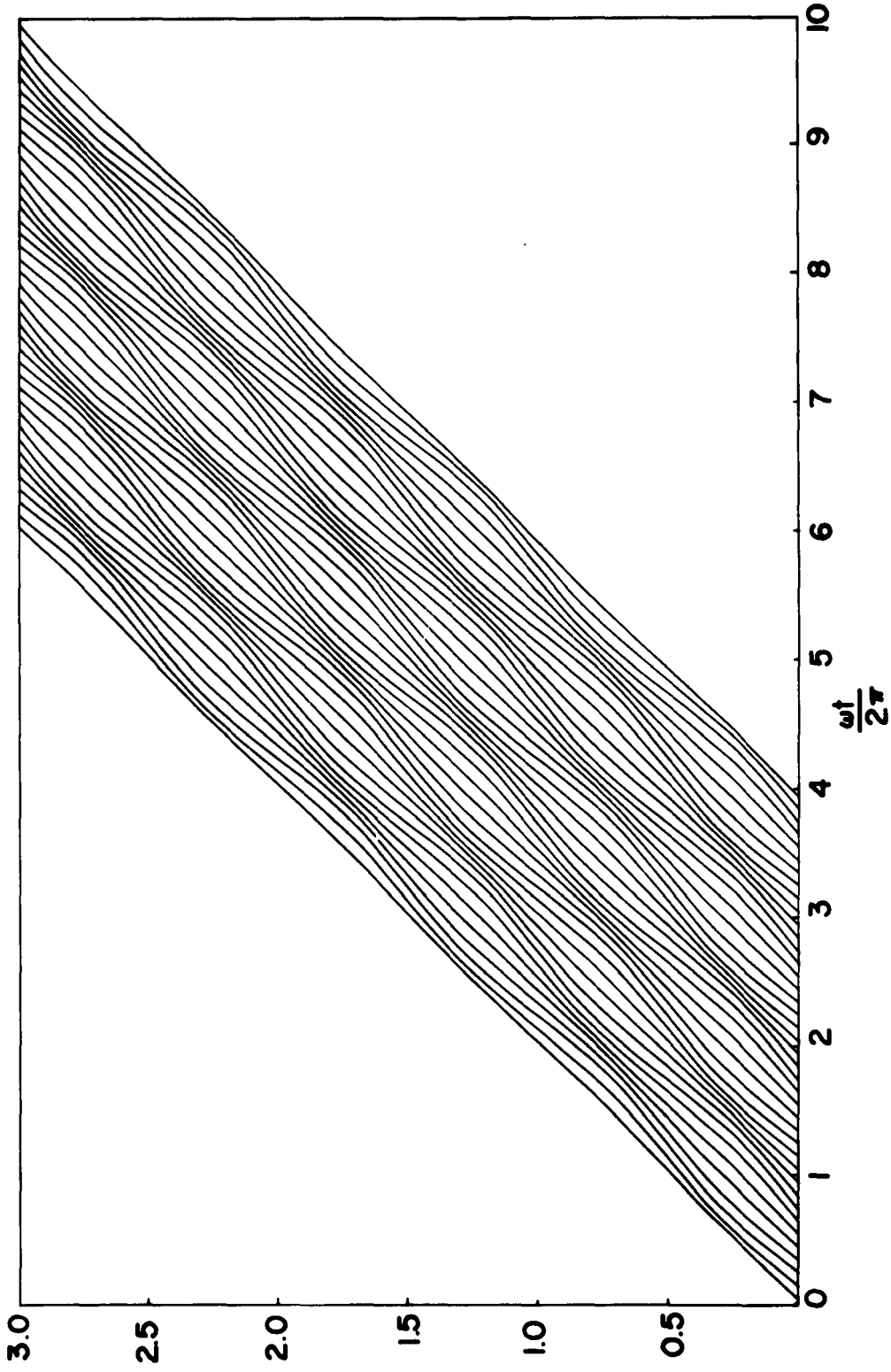

Figure 15. $\frac{\varepsilon_e}{\varepsilon_p} = 2.0$

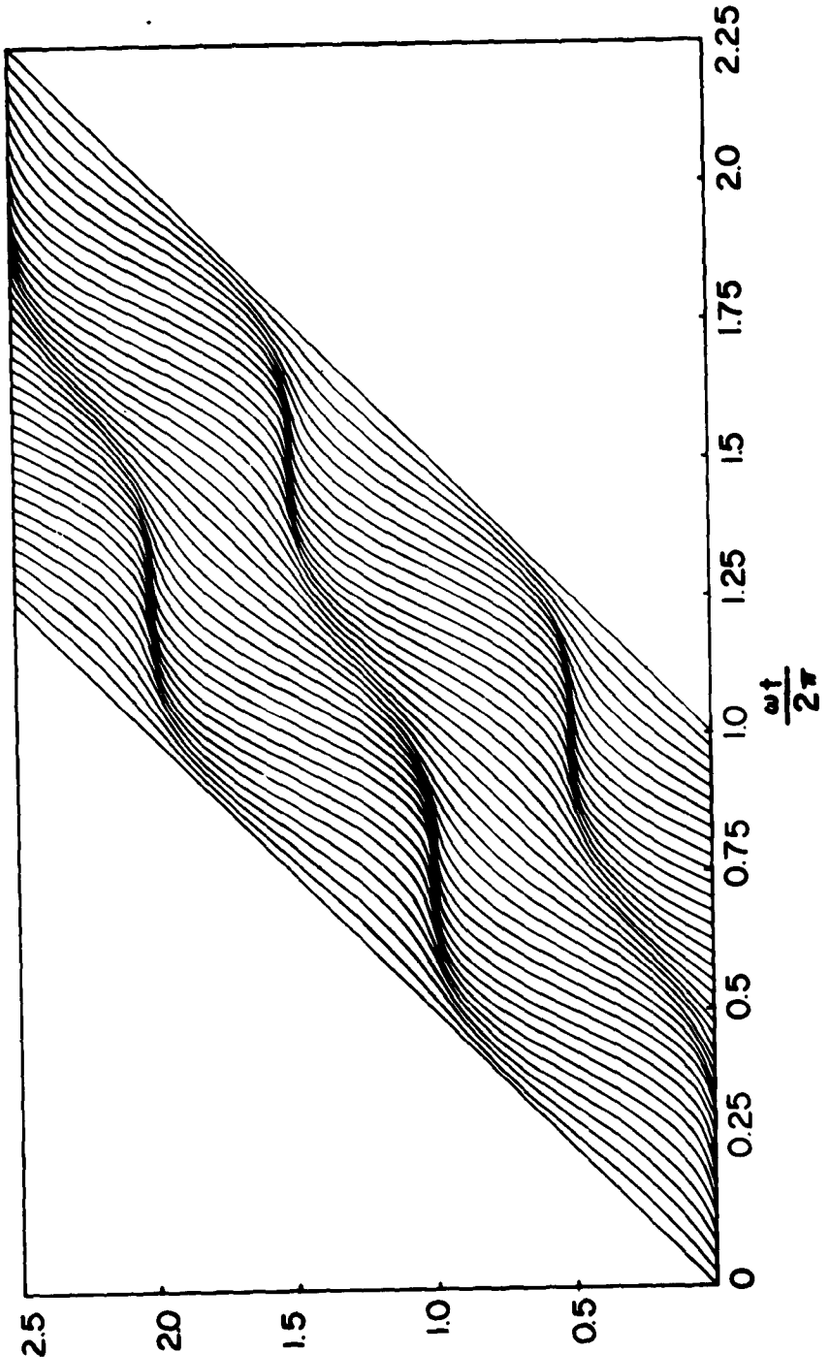

Figure 16. $\frac{\omega}{\omega_p} = 1.0$

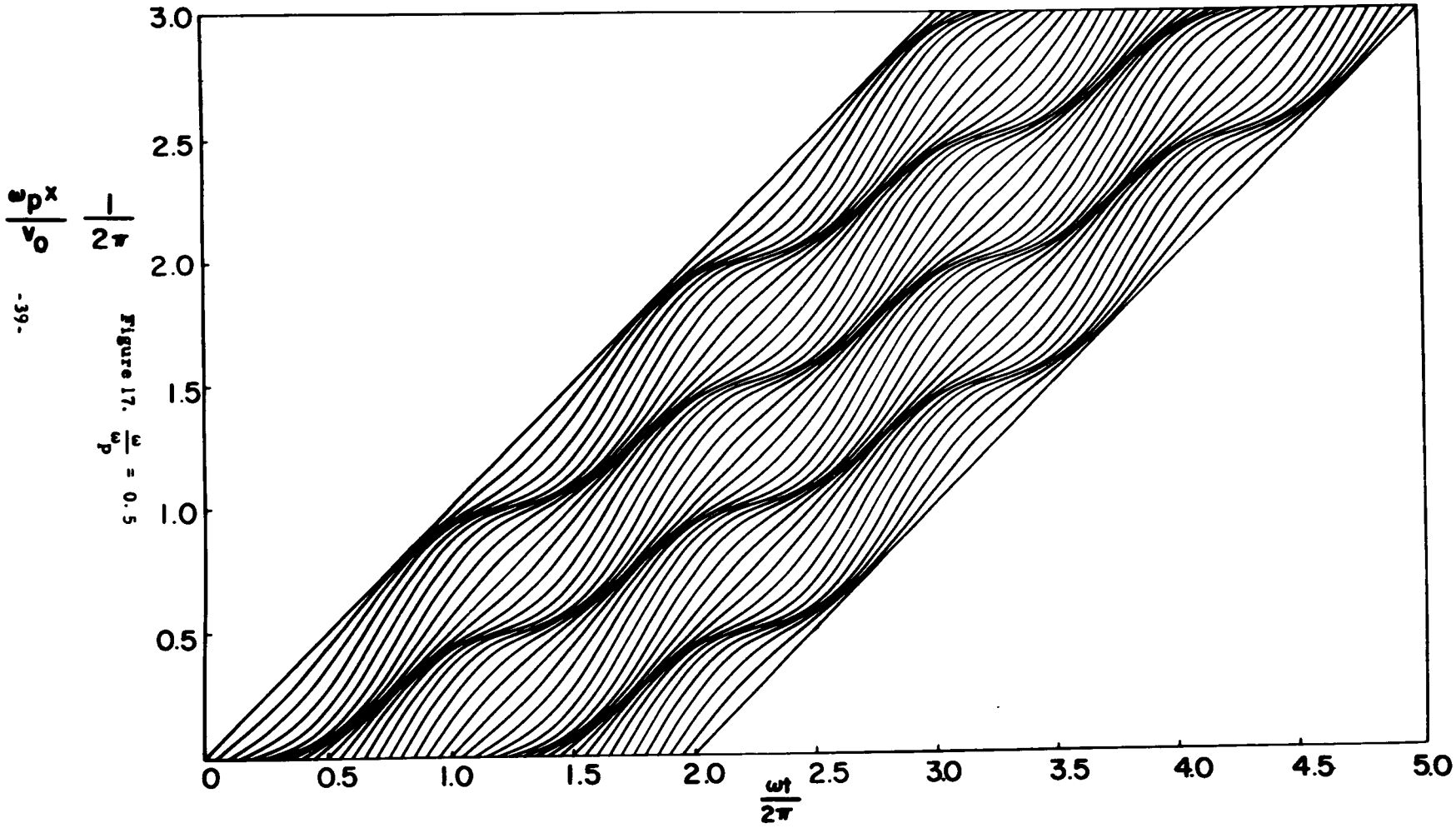
3.0
2.5
2.0
1.5
1.0
0.5
0
0.5
1.0
1.5
2.0
2.5
3.0
3.5
4.0
4.5
5.0
$\frac{\omega_p x}{v_0} \frac{1}{2\pi}$
$\frac{\omega t}{2\pi}$
$\omega_p/\omega = 0.5$

Figure 17.

CURRENT MODULATION

In the case of current modulation only, the displacement is

$$\frac{\omega_p}{v_o} x(t, t_a) = \omega_p (t - t_{oa}) + \frac{i_1}{i_o} \frac{\omega_p}{\omega} \sin (\omega t_a - \phi) \cos \omega_p (t - t_a) \tag{1}$$

This may be compared with the case for velocity modulation. Let the preceding t_a time axis be shifted so that $(\omega t_a - \phi)$ becomes $(\omega t_a' + \pi/2)$. Let the $(t-t_a)$ axis be shifted so that $\left[\omega_p (t - t_a)\right]$ becomes $\left[\omega_p(t' - t_a') - \pi/2.\right]$. The new displacement is

$$\frac{\omega_p x}{v_o} (t', t_a') = \omega_p (t' - t'_{oa}) - \pi/2 + \frac{i_1}{i_o} \frac{\omega_p}{\omega} \cos \omega_a' \quad \sin \omega_p(t' - t_a') \tag{2}$$

This is the same form as for velocity modulation, but shifted in time and displaced $\pi/2$ in normalized distance $(\lambda_p/4)$. Hence, new plots are unnecessary.

INTERACTION WITH A TRAVELING WAVE

The stream may react to its own fields, space-charge fields, and may also be driven by externally applied fields. Such fields, of course, are necessary to provide the initial modulation, v_1 and i_1, used earlier; these fields presumably are imposed over a short length of stream, a diode or gap region. Particle motion in a gap has been given in great detail by many authors over the past three decades, as found in the classical monograph by Llewellyn (1941) and as outlined by one of the earliest workers with transit time effects, Benham, in Benham and Harris (1957).

Interaction with a traveling wave provides an interesting example of a driven stream, as well as insight into the initial bunching process in a traveling-wave tube. The problem solved here is very simple and somewhat non-physical. A slow wave of phase velocity v_p is caused to travel with a stream of average velocity v_o. The wave produces bunching and may alter

the stream kinetic energy; this change in kinetic energy will appear in field energy, some of which may cause the driving wave to increase (as in a traveling-wave tube) or decrease (as in an accelerator), all as a self-consistent process. However, here, only the initiation of bunching will be obtained because the driving field will be taken to be constant.

The electric field of the driving wave is given in terms of laboratory coordinates as,

$$E_w(x, t) = E_w \sin\left(\omega t - \frac{\omega x}{v_p}\right) \tag{1}$$

The equation of motion for a particle is

$$\frac{m\,\partial^2 x}{\partial t^2} = e\,E_{\text{space charge}} + e\,E_{\text{wave}} \tag{2}$$

where the fields are given at the particle. The particle position x appears in E_{wave}, whereas solution would be easier if the equilibrium position x_o appeared. Hence, one may expand E_w as

$$E_w(x, t) = E_w(x_o, t) + \frac{\partial E_w(x_o, t)}{\partial x}(x - x_o) + - - - \tag{3}$$

$$= E_w \sin\left(\omega t - \frac{\omega x_o}{v_p}\right) - \frac{\omega}{v_p}(x - x_o) E_w \cos\left(\omega t - \frac{\omega x_o}{v_p}\right) + - - - \tag{4}$$

The phase is

$$\frac{\omega}{v_p}(x - x_o) = 2\pi \frac{x - x_o}{\lambda_w} \tag{5}$$

where λ_w is the wavelength of the driving wave. In the limit of small excitation, the deviation $x - x_o$ will be much smaller than λ_w, so that the second term may be ignored. The problem solved is for no initial current modulation and no initial velocity modulation. Thus, $t_{oa} = t_a$. Hence

$$x_o = v_o(t - t_a) \tag{6}$$

Thus, the phase of E_w becomes

$$\omega t - \frac{\omega x}{v_p} = \omega t - \frac{\omega v_o}{v_p}(t - t_a) \tag{7}$$

$$= \omega\left(1 - \frac{v_o}{v_p}\right)t + \frac{v_o}{v_p}\,\omega t_a \tag{8}$$

$$= \omega' t + \frac{v_o \omega t_a}{v_p} \tag{9}$$

ω' is the frequency of the wave as seen by the stream, the usual Doppler shifted value. The response of the stream to the wave is expected to be greatest if ω' is at the resonant frequencies of the stream, $\pm \omega_p$, or

$$\omega\left(1 - \frac{v_o}{v_p}\right) = \pm \omega_p \tag{10}$$

$$\frac{\omega}{v_p} = \frac{\omega}{v_o} \mp \frac{\omega_p}{v_o} \tag{11}$$

That is, greatest response is expected if the wave velocity is that of the faster or the slower space-charge wave. Physically this requires that the wave should move one wavelength past the stream in one cycle of the plasma frequency; this slip is just that used to obtain maximum growth rate in traveling-wave tubes with moderate-to-large space-charge densities. Choosing this synchronism, one obtains the equation of motion,

$$\frac{\partial^2 x}{\partial t^2} + \omega_p^2 (x - x_o) = \frac{e}{m} E_w \sin\left[\pm \omega_p (t - t_a) + \omega t_a\right] \tag{12}$$

The solution is

$$x(t, t_a) = x_o - \frac{\frac{e}{m}E_w}{2\omega_p^2}\left\{\pm \omega_p (t - t_a) \cos\left[\pm \omega_p (t - t_a) + \omega t_a\right]\right.$$

$$\left. - \cos \omega t_a \sin\left[\pm \omega_p (t - t_a)\right]\right\} \tag{13}$$

The $\omega_p(t-t_a)$ term shows the growth of displacement from equilibrium due to traveling-wave interaction, increasing linearly with time of flight; however, the motion is still oscillatory, with electrons sliding through the bunches and not being trapped. If the synchronism is with the slower space-charge wave (lower sign), then, bunches will be formed in the retarding phase of E_w; this implies decrease of kinetic energy of the stream and increase of wave energy, that is, an increase in E_w. Had an energy balance been required, E_w would grow. Then, in turn $x-x_o$ would grow even more rapidly, as would E_w, resulting in the usual exponential growth. Similarly, for synchronism with the faster space-charge wave, bunches are formed in the accelerating phase and E_w must decrease, as in an accelerator.

Solutions of the self-consistent problem would be more useful. Also, in either solution, as the deflection grows, particles must cross at some point so that complete solution to maximum growth of the wave or stream energy virtually requires use of a high speed computer; typical machine solutions and trajectories are given by Tien (1955).

HISTORICAL NOTE; ACKNOWLEDGMENT

Distance-time plots are quite commonly made for one-dimensional problems. Perhaps the most well-known electron stream plot is that for the klystron as drawn by a patent lawyer, Applegate (1942), for the early Varian-Hansen klystron patent applications. In his drawing, space-charge forces were neglected. There is the temptation to use the Eulerian space-charge wave solutions as a guide to altering the Applegate diagram so as to show the effect of space-charge forces. These efforts generally fail with the common and easily-detected error of putting the turnaround points at $\lambda_{p/4}$. The particle trajectories shown here were initially solved for and sketched by J. L. Palmer for a graduate seminar given by the writer at the University of California, Berkeley, in 1959. A proper name for them would be Palmer diagrams. The derivation given here is somewhat different, following the classical Lagrangian form as used by Benham (1928) and Llewellyn (1941) for diode problems. However, many steps here are parallel to those of Palmer to whom the writer is most grateful. The drawings shown are due to the computing of R. Lanstein, the careful plotting by Betty Jean Hansen and the skilled drawing of George Faraco.

REFERENCES

1928 Benham, W. E., "Theory of the Internal Action of Thermionic Systems at Moderately High Frequencies", Part I Phil. Mag. (March 1928); Part II, Phil. Mag. Supp. II (February 1931).

1939 Hahn, W. C., "Small Signal Theory of Velocity-Modulated Electron Beams, Gen. Elec. Rev. 42, 258-270, June.

Hahn, W. C., "Wave Energy and Transconductance of Velocity-Modulated Electron Beams", Gen. Elec. Rev. 42, 497-502, November.

Ramo, S., "The Electronic-Wave Theory of Velocity Modulation Tubes", Proc. IRE 27 757-763, December.

1941 Llewellyn, F. B., Electron-Inertia Effects, Cambridge Univ. Press, Cambridge, England.

1942 Applegate, L. M.; see for example Figure 3E U. S. Patent No. 2, 269, 456, W. W. Hansen, R. H. Varian, January 13, (Filed January 22, 1938).

1955 Tien, P. K., Walker, L. R., Wolontis, V. M., "A Large Signal Theory of Traveling Wave Amplifiers", Proc. IRE 43 260-276, March.

1957 Benham, W. E., and Harris, I. A., The Ultra High Frequency Performance of Receiving Tubes, McGraw-Hill Book Co., Inc., N. Y.

1959 Dawson, John. "Nonlinear Electron Oscillations in a Cold Plasma", Phys. Rev. 113 383-387, January 15.

1960 Jackson, E. A., "Non-Linear Oscillations in a Cold Plasma", Physics of Fluids, 3 831-833, September-October.

AIR FORCE OFFICE OF SCIENTIFIC RESEARCH
ELECTRON TUBE RESEARCH
CONTRACT NO. AF 49(638)-102

DISTRIBUTION LIST

ADDRESSEE	NO COPIES
AFOSR ATTN: Technical Library Washington 25, D C	2
AFOSR (SRPP) Washington 25 D C	1
ASD ATTN Technical Library Wright Patterson AFB Ohio	1
AFCRL ATTN Technical Library L G Hanscom Field Bedford Massachusetts	1
EOAR The Shell Building 47 Rue Cantersteen Brussels Belgium	(Unclassified Reports) 1
ARL ATTN Technical Library Wright Patterson AFB Ohio	1
ASTIA (TIPCR) Arlington Hall Station Arlington 12 Virginia	10
Director of Research Headquarters USAF ATTN AFRDR Washington 25 D C	1
Office of Naval Research Department of the Navy ATTN Code 420 Washington 25 D C	1
Naval Research Laboratory ATTN Technical Library Washington 25 D C	1
Chief Research and Development ATTN Scientific Information Branch Department of the Army Washington 25 D C	1
Chief, Physics Branch Division of Research U S Atomic Energy Commission Washington 25 D C	1
U S Atomic Energy Commission Technical Information Extension P O Box 62 Oak Ridge Tennessee	1
National Bureau of Standards ATTN Technical Library Room 203, Northwest Building Washington 25 D C	1
Physics Program National Science Foundation Washington 25, D C	1
Director, Army Research Office Durham Box CM, Duke Station Durham, North Carolina	1
AEDC (AEOIM) ATTN Technical Library Arnold Air Force Station Tullahoma, Tennessee	1
AFFTC (AFOTL) ATTN: Technical Library Edwards AFB California	1
AFMDC (MDF) Holloman AFB, New Mexico	1
AFMDC (HDOI) Holloman AFB New Mexico	1
ARGMA (ORDXR-OTL) Redstone Arsenal, Alabama	1
Institute of Technology (AU) Library MCLI-LIB, Bldg 125, Area B Wright-Patterson AFB Ohio	1
AFSC (SCRS) Andrews AFB Washington 25, D C	1
Signal Corps Engineering Laboratory ATTN (SIGFM/EL-RPO) Fort Monmouth, New Jersey	1
Headquarters National Aeronautics and Space Administration ATTN: Technical Library Washington 25, D C	1
Ames Research Center (NASA) ATTN: Technical Library Moffett Field, California	1
Technical Information Division Bldg. 50, Room 101 Radiation Laboratory Berkeley, California	1
Hans Motz Oxford University Oxford, England	1
Miss May Dorin Department of Archives 303 Library University of California Berkeley 4, California	1
High Speed Flight Station (NASA) ATTN Technical Library Edwards AFB California	1
Langley Research Center (NASA) ATTN Technical Library Langley AFB California	1
Lewis Research Center (NASA) ATTN Technical Library 21000 Brookpark Road Cleveland 35 Ohio	1
Goddard Space Flight Center (NASA) ATTN Technical Library Greenbelt, Maryland	1
George C Marshall Space Flight Center (NASA) ATTN Technical Library Redstone Arsenal, Alabama	1
Wallops Station (NASA) ATTN Technical Library Wallops Island Virginia	1
Institute of Aeronautical Sciences 2 East 64th Street New York 21 New York	(Unclassified Reports) 1
Applied Mechanics Reviews Southwest Research Institute 8500 Culebra Road San Antonio 6 Texas	(Unclassified Reports) 1
Linda Hall Library ATTN Document Division 5109 Cherry Street Kansas City 10 Missouri	(Unclassified Reports) 1
AFOSR (SRAL) ATTN Technical Library Holloman AFB New Mexico	2
AFSWC (SWOI) Kirtland AFB New Mexico	1
Advanced Research Projects Agency Washington 25 D C	1
Rand Corporation 1700 Main Street Santa Monica, California	1
Chairman Canadian Joint Staff (DRB/DSIS) 2450 Massachusetts Avenue, N W Washington 25, D C	*Unclassified Reports 1
Officer in Charge Office of Naval Research Navy No 100 Fleet Post Office New York New York	1
Office of Technical Services Department of Commerce Technical Reports Branch Washington 25 D C	1
M D Adcock Head American Systems Incorporated 1625 E 126 Street Hawthorne California	1
Dr Harold Glaser Office of Naval Research Washington 25, D C	1
Professor Charles Townes Department of Physics Columbia University New York 27 New York	1
Professor Harvey Brooks Department of Physics Harvard University Cambridge 38, Massachusetts	1
Professor P Kusch Department of Physics Columbia University New York 27, New York	1
Professor N Bloembergen Department of Physics Harvard University Cambridge 38 Massachusetts	1
Dr Irving Rowe Office of Naval Research 346 Broadway New York, New York	1
W A Kozumplik, Manager Lockheed Aircraft Corporation Missiles and Space Division Technical Information Center 3251 Hanover Street Palo Alto, California	1
Mr F Ohrese Sperry Gyroscope Company Electron Tube Division Mail Station 1 B40 Great Neck, New York	1
DOFL (ORDTL 012) Washington 25, D C	1
Prof J H Mulligan, Jr Chairman, Department of Electrical Engineering New York University 25 Waverly Place New York, New York	1
The Ohio State University Antenna Laboratory 2024 Neil Avenue Columbus 10, Ohio ATTN Security Officer	1
Major General Casemiro Montenegro Filho Central Technico da Aeronáutica (CTA) São José dos Campos São Paulo, Brazil	1
Purdue University Lafayette, Indiana ATTN Richard L Funkhouser Engineering Librarian	1
Professor J Van Bladel Electrical Engineering Department College of Engineering University of Wisconsin Madison 6, Wisconsin	1
Professor W Low Department of Physics The Hebrew University of Jerusalem Jerusalem, Israel	1
University of Illinois Department of Electrical Engineering Urbana Illinois ATTN H Von Foerster	1
Ohio State University Department of Electrical Engineering Columbus Ohio	1
The University of Michigan Department of Electrical Engineering Electron Physics Laboratory Ann Arbor Michigan ATTN Professor J E Rowe	1
Stanford University Electronics Research Laboratory Stanford California	1
Massachusetts Institute of Technology Research Labs of Electronics Room 20H 22c, Document Office Cambridge 39, Massachusetts ATTN J. H. Hewitt	1
Harvard University Cruft Laboratory Cambridge 38 Massachusetts ATTN Technical Reports Collection	1
Technical Information Libraries Bell Telephone Laboratories, Inc Whippany Laboratory Whippany, New Jersey ATTN Technical Reports Librarian	1
California Institute of Technology Pasadena 4, California ATTN R Gould	1
Sylvania Electric Company Mountain View, California ATTN D H Goodman	1
Professor William H Surder Electrical Engineering Department Princeton University Princeton, New Jersey	1
General Electric Company Electron Tube Div of the Research Lab The Knolls Schenectady, New York ATTN E D McArthur	1
General Electric Company Missile and Space Vehicle Department 3198 Chestnut Street Philadelphia 4, Pennsylvania ATTN Aerodynamics Engineering Operation R F Peck, Manager	1
Hughes Aircraft Company Florence at Teale Street Culver City, California ATTN: Documents Group Bldg 6, Rm X2015	1
RCA Laboratories Princeton, New Jersey ATTN Dr W M Webster, Director Electronics Research Labs	1
Varian Associates 611 Hansen Way Palo Alto, California ATTN: Technical Library	1
Westinghouse Electric Corporation Electronic Tube Division P O Box 284 Elmira, New York ATTN: Mr Sheldon S King, Librarian	1
Professor Zohrab Kaprielian University of Southern California School of Engineering Department of Electrical Engineering University Park Los Angeles 7, California	1
R J Maxum Dalmo Victor Research Laboratories Belmont California	1
Headquarters Air Force Office of Scientific Research Office of Aerospace Research USAF Washington 25, D C. ATTN: Marshall C Harrington General Physics Division	1